Two-loop functional renormalization group of the random field and random anisotropy $O(N)$ models

Matthieu Tissier* and Gilles Tarjus†
LPTMC, CNRS-UMR 7600, Université Pierre et Marie Curie, Boîte Postale 121, 4 Pl. Jussieu, 75252 Paris Cédex 05, France
(Received 27 June 2006; published 18 December 2006)

We study by the perturbative functional renormalization group (FRG) the random field and random anisotropy $O(N)$ models near $d=4$, the lower critical dimension of ferromagnetism. The long-distance physics is controlled by zero-temperature fixed points at which the renormalized effective action is nonanalytic. We obtain the beta functions at two-loop order, showing that despite the nonanalytic character of the renormalized effective action, the theory is perturbatively renormalizable at this order. The physical results obtained at the two-loop level, most notably concerning the breakdown of dimensional reduction at the critical point and the stability of quasi-long-range order in $d<4$, are shown to fit into the picture predicted by our recent nonperturbative FRG approach.

DOI: 10.1103/PhysRevB.74.214419 PACS number(s): 75.40.Cx, 11.10.Hi

I. INTRODUCTION

Despite decades of intensive investigation the effect of weak quenched disorder on the long-distance physics of many-body systems remains in part an unsettled problem. This is the case for the class of models in which N-component classical variables with $O(N)$ symmetric interactions are coupled to a random field. Depending on whether the coupling is linear or bilinear, the models belong to the "random field" (RF) or the "random anisotropy" (RA) subclasses. Such models with $N=1$, 2, or 3 are relevant to describe a variety of systems encountered in condensed matter physics or physical chemistry. To name a few, one can mention dilute antiferromagnets in a uniform magnetic field,[1] critical fluids and binary mixtures in aerogels (both systems being modeled by the $N=1$ RF Ising model),[2–4] vortex phases in disordered type-II superconductors (described in terms of an elastic glass model whose simplest version is the $N=2$ RF XY model),[5–9] amorphous magnets, such as alloys of rare-earth compounds,[10,11] and nematic liquid crystals in disordered porous media (described by $N=2$ or $N=3$ RA models).[12]

On the theoretical side the main questions raised about the equilibrium behavior of such systems concern the nature and the characteristics of the phases and of the phase transitions. It has been shown by both heuristic and rigorous methods[13–17] that the lower critical dimension below which no long-range order is possible is $d_{lc}=2$ for the RFIM and $d_{lc}=4$ for RF models with a continuous symmetry [$O(N)$ with $N>1$]. The same conclusion applies to RA models with the restriction that only ferromagnetic (to use a magnetic terminology) long-range order is forbidden below $d_{lc}=4$; another type of long-range order associated to a spin-glass phase is still possible.[11] Here, we only consider RA models with isotropic distributions of the random anisotropies and with $N>1$; for anisotropic distributions, long-range ferromagnetic ordering may still occur below $d_{lc}=4$, whereas RA makes no real sense for $N=1$, the model reducing then either to the random temperature Ising model or to the pure Ising model depending on the details of the effective Hamiltonian.[11]

Two central issues remain under active debate. The first one is about the so-called "dimensional reduction" property. Standard perturbation theory predicts to all orders that the critical behavior of an $O(N)$ model in the presence of RF is the same as that of the pure model, i.e., with no RF, in two dimensions less.[18] The same applies to the RA$O(N)$M with $N>1$ near the paramagnetic-ferromagnetic transition.[19] Dimensional reduction is known, however, to break down, its most striking failure being the prediction of a lower critical dimension $d_{lc}=3$ for the RFIM in contradiction with the exact result (see above). A proper description of the long-distance behavior of RF and RA models must thus provide a way out of the dimensional reduction.

The second issue concerns the phase diagram of the RF and RA models with a continuous symmetry ($N>1$) in dimensions below $d=4$, which of course are relevant to the physical situations. If long-range ferromagnetism is forbidden, quasi-long-range order (QLRO), namely a phase characterized by no magnetization and a power-law decrease of the correlation functions at large distances, may still exist.[5–9,20] It has been shown that QLRO is absent for $N \geqslant 3$ in the presence of RF and for $N \geqslant 10$ in the presence of RA;[20] yet it has been argued that QLRO is present for $N=2$ in $d=3$, in which case it corresponds to the "Bragg glass" phase predicted for vortices in disordered type-II superconductors.[5,8,9]

We have recently proposed a coherent resolution of those issues based on a nonperturbative (NP) functional renormalization group (FRG) treatment.[21,22] This approach has allowed us to provide a unified picture of ferromagnetism, QLRO, and criticality in RF models in the whole (N,d) diagram as well as a way to escape dimensional reduction.

The main findings[21,22] can be summarized on the phase diagram of the RF$O(N)M$ shown in Fig. 1. In region III, there are no phase transitions and the system is always disordered (paramagnetic). In regions I and IV, there is a second-order paramagnetic to ferromagnetic transition and in region II, a second-order transition between paramagnetic and QLRO phases. In all cases, the critical behavior is controlled by a zero-temperature fixed point at which temperature is formally irrelevant. At this fixed point the *renormal-*

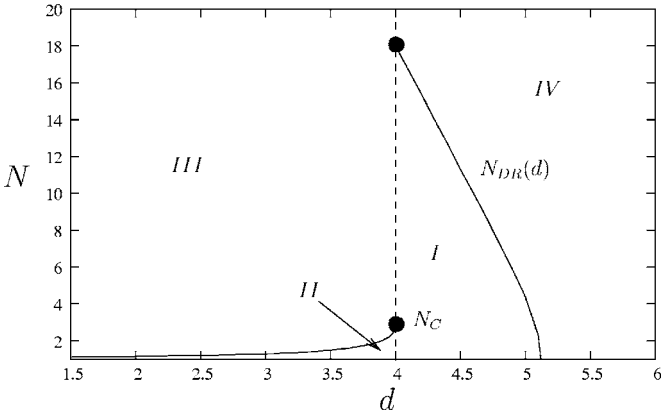

FIG. 1. Nonperturbative FRG prediction for the (N,d) phase diagram of the RF$O(N)M$. See text for comments.

ized effective action is a nonanalytic function of its arguments (the order parameter fields). Although present, the nonanalyticity is weak enough in region IV to let the critical exponents take their dimensional reduction value (corrections to scaling may nonetheless differ from the dimensional reduction predictions). In regions I and II the nonanalyticity takes the form of a cusp in the renormalized second cumulant of the random field, which leads to a complete breakdown of dimensional reduction. Finally, the whole QLRO phase in region II is also controlled by a zero-temperature fixed point characterized by a cusp.

There is undoubtedly room for improving the quantitative predictions of our NP-FRG theory, in terms of both the number of observables studied and, more importantly, of the accuracy of the (necessary) approximations involved. (In addition, the NP-FRG study of the RA$O(N)M$ has not yet been completed.) The robustness of the proposed scenario may, however, be tested by considering a *perturbative* FRG treatment of the models near $d=4$. Such a perturbative FRG has been pioneered by D. Fisher[19,23] and widely used to study the statics and the depinning of elastic systems pinned by quenched disorder.[5,8,9,24,25]

At one-loop level, the flow equation for the renormalized second cumulant of the disorder, first derived by Fisher[19] for the RF and RA $O(N)$ models, has been studied by several authors.[20–22,26,27] The results fit into the diagram displayed in Fig. 1, which should come as no surprise: the flow equations obtained in our NP-FRG approach exactly reproduce the one-loop result near $d=4$.[22] Below, we give a survey of the behavior of the RF$O(N)M$ at the one-loop level in $d=4+\varepsilon$, including some new results, as well as a study of the related RA$O(N)M$.

To go beyond this first step, one must consider the next order in the loop expansion. However, the technical difficulties are now much more involved than at the one-loop level. On top of the rapidly increasing number of diagrams, diagrams which in the present case are functionals, the nonanalytic character of the renormalized effective action at $T=0$ leads to the appearance of "anomalous" terms in the diagramatics, whose evaluation is *a priori* ambiguous. A resolution of the problem has been proposed for the simpler case of disordered elastic systems by Le Doussal, Wiese, and co-workers.[25]

A preliminary account of this work has been published in Ref. 21. An independent calculation has appeared in Ref. 30.

The rest of the paper is organized as follows. In Sec. II we present the RF and RA $O(N)$ models and their nonlinear sigma versions appropriate to describe the long-distance physics near the lower critical dimension of ferromagnetism, $d=4$. We outline the perturbative FRG framework and the way to extract scaling behavior and critical exponents. Section III is devoted to an analysis of the one-loop FRG equations at $T=0$ in $d=4+\epsilon$, discussing the fixed points and their stability and contrasting the RF and RA cases. In Sec. IV we derive the FRG beta functions at two-loop order in $T=0$. We present the diagrammatic representation and the method used to handle the apparent ambiguities appearing in the formulation due to the nonanalytic character of the renormalized dimensionless effective action. Proceeding in this way we obtain a well-defined renormalized theory at two-loop order. The physical results obtained from solving the two-loop FRG equations are discussed in Sec. V, and we stress the new features appearing at this order. Several technical aspects of the work are deferred to Appendixes.

II. MODELS AND FRAMEWORK

A. Models

We consider the $O(N)$ model in the presence of RF or RA near $d=4$. We stress again that $d=4$ is the lower critical dimension for $N>1$ and for the paramagnetic-to-ferromagnetic transition. In a manner similar to that developed for the pure model at low temperature near $d=2$, the long-distance physics for weak disorder (which, we recall, takes here the role played by low temperature in the pure model, temperature being now irrelevant and eventually set to zero) can be described in a field-theoretical setting by a nonlinear sigma model with effective Hamiltonian

$$\mathcal{H}[\mathbf{S}] = \int d^dx \frac{1}{2}[\nabla \mathbf{S}(\mathbf{x})]^2 - \sum_i [h^i(\mathbf{x}) + H\hat{u}^i]S^i(\mathbf{x}) - \sum_{ij} \tau^{ij}(\mathbf{x})S^i(\mathbf{x})S^j(\mathbf{x}), \quad (1)$$

where the N-component spins $\mathbf{S}$ satisfy the fixed-length constraint, $\mathbf{S}(\mathbf{x})^2=1$, and $\mathbf{H}=H\hat{\mathbf{u}}$ is a uniform external magnetic field; $\mathbf{h}(\mathbf{x})$ is a random magnetic field and $\tau(\mathbf{x})$ a second-rank random anisotropy tensor, both with Gaussian distributions characterized by zero means and variances given by

$$\overline{h^i(\mathbf{x})h^j(\mathbf{y})} = \Delta\,\delta_{ij}\delta(\mathbf{x}-\mathbf{y}), \quad (2)$$

$$\overline{\tau^{ij}(\mathbf{x})\tau^{kl}(\mathbf{y})} = \frac{\Delta_2}{2}(\delta_{ik}\delta_{jl} + \delta_{il}\delta_{jk})\,\delta(\mathbf{x}-\mathbf{y}). \quad (3)$$

Higher-order random anisotropies could be included as well. They will indeed be generated in the perturbation expansion and the renormalization group flow.[19] However, starting with only a second-rank (or more generally an even-rank) random anisotropy, only even-rank anisotropies will be generated. In what follows we will therefore use the acronym RA to characterize models with even-rank random anisotropies.

From the associated partition function,

$$\mathcal{Z} = \int \mathcal{D}\mathbf{S}\,\delta(\mathbf{S}^2 - 1)\exp\left(-\frac{1}{T}\mathcal{H}[\mathbf{S}]\right), \tag{4}$$

one can obtain the free energy by averaging the logarithm of $\mathcal{Z}$ over the quenched disorder. This is more conveniently performed by introducing replicas $\mathbf{S}_a(\mathbf{x})$, $a=1,\ldots,n$, which leads after explicitly performing the average over the disorder to the following "replicated" effective Hamiltonian

$$\mathcal{H}_n[\{\mathbf{S}_a\}] = \int d^dx \sum_a \frac{1}{2}[\nabla \mathbf{S}_a(\mathbf{x})]^2 - \sum_a H\hat{\mathbf{u}}\cdot\mathbf{S}_a(\mathbf{x}) - \frac{1}{2T}\sum_{ab} R_0[\mathbf{S}_a(\mathbf{x})\cdot\mathbf{S}_b(\mathbf{x})] \tag{5}$$

with

$$R_0(z) = \Delta z + \Delta_2 z^2 \tag{6}$$

and $-1 \leqslant z \leqslant +1$. The fluctuations around a fully ordered state in which spins in all replicas align in the same direction are as usual handled by splitting the replica field $\mathbf{S}_a(\mathbf{x})$ into a component collinear to the external field (and to the magnetization), $\Sigma_a(\mathbf{x}) = \mathbf{S}_a(\mathbf{x})\cdot\hat{\mathbf{u}}$, and $N-1$ components orthogonal to it, $\mathbf{\Pi}_a(\mathbf{x}) = \mathbf{S}_a(\mathbf{x}) - \Sigma_a(\mathbf{x})\hat{\mathbf{u}}$. By using the relation between $\Sigma_a(\mathbf{x})$ and $\mathbf{\Pi}_a(\mathbf{x})$ imposed by the unit-length constraint, the replicated partition function can be expressed as a functional integral over the $(N-1)$-component replica fields $\mathbf{\Pi}_a(\mathbf{x})$,

$$\mathcal{Z}_n = \int \prod_a \mathcal{D}\mathbf{\Pi}_a \times \exp\left(-\sum_a \mathcal{S}_1[\mathbf{\Pi}_a] + \frac{1}{2}\sum_{ab}\mathcal{S}_2[\mathbf{\Pi}_a,\mathbf{\Pi}_b] + \cdots\right), \tag{7}$$

where the 1-replica and 2-replica parts of the action read

$$\mathcal{S}_1[\mathbf{\Pi}_a] = \frac{1}{T}\int d^dx \left\{\frac{1}{2}(\nabla\mathbf{\Pi}_a)^2 + \frac{(\mathbf{\Pi}_a\cdot\nabla\mathbf{\Pi}_a)^2}{2(1-\mathbf{\Pi}_a^2)} - H\sqrt{1-\mathbf{\Pi}_a^2}\right\}, \tag{8}$$

$$\mathcal{S}_2[\mathbf{\Pi}_a,\mathbf{\Pi}_b] = \frac{1}{T^2}\int d^dx R_0(\mathbf{\Pi}_a\cdot\mathbf{\Pi}_b + \sqrt{1-\mathbf{\Pi}_a^2}\sqrt{1-\mathbf{\Pi}_b^2}) \tag{9}$$

and the dots denote terms, such as those produced by the Jacobian of the transformation from the $\mathbf{S}_a$'s to the $\mathbf{\Pi}_a$'s and possible contributions involving more than two replicas, that either do not contribute to the perturbation expansion in the $T=0$ limit or turn out to be irrelevant within conventional power counting.[19,25]

From the logarithm of the partition function, Eq. (7), one can obtain, by a Legendre transform with respect to external sources coupled to the $(N-1)$-component replica fields $\mathbf{\Pi}_a(\mathbf{x})$, the effective action $\Gamma_n[\{\mathbf{\Pi}_a\}]$ which is the generating functional of the one-particle irreducible vertices for the $\mathbf{\Pi}_a$ fields and from which all equilibrium observables can be derived. (The subscript n will be dropped in the following.)

B. Perturbation theory and renormalization

We proceed by calculating the effective action $\Gamma[\{\mathbf{\Pi}_a\}]$ perturbatively in powers of the disorder correlator R_0, keeping only terms that do not vanish in the limit $T=0$. The results so obtained would, however, be singular, showing the standard ultraviolet divergences as $\epsilon = d-4$ goes to zero. For instance, if we use the dimensional regularization as a regularization scheme, the one-loop calculation brings in terms proportional to $1/\epsilon$. To cure this problem, it is necessary to renormalize the theory by introducing in the effective Hamiltonian "counterterms" that are chosen to keep the physical quantities finite.

Expressed in terms of dimensionless renormalized quantities at an arbitrary momentum scale μ, the 1- and 2-replica parts of the action read:

$$\mathcal{S}_1[\pi_a] = \frac{\mu^{d-2}Z_\Pi}{2Z_T t}\int d^dx \left\{(\nabla\pi_a)^2 + Z_\Pi\frac{(\pi_a\cdot\nabla\pi_a)^2}{1-Z_\Pi\pi_a^2} - 2Z_\Pi^{1/2}Z_T h\sqrt{1-Z_\Pi\pi_a^2}\right\}, \tag{10}$$

$$\mathcal{S}_2[\pi_a,\pi_b] = \frac{\mu^d}{2Z_T^2 t^2}\int d^dx Z_R(z_0 = Z_\Pi\pi_a\cdot\pi_b + \sqrt{1-Z_\Pi\pi_a^2}\sqrt{1-Z_\Pi\pi_b^2}), \tag{11}$$

where the dimensionless renormalized quantities are defined as

$$\mathbf{\Pi} = \sqrt{Z_\Pi}\pi, \tag{12a}$$

$$T = \mu^{2-d}Z_T t, \tag{12b}$$

$$H = Z_T Z_\Pi^{-1/2} h, \tag{12c}$$

$$R_0 = \mu^{4-d}Z_R, \tag{12d}$$

and $Z_R(z)$ is a functional of the renormalized dimensionless disorder correlator $R(z)$, with its leading term equal to $R(z)$. The two renormalization constants Z_T and Z_Π and the renormalization function $Z_R(z)$ are chosen so that the loopwise perturbative expansion of the effective action remains finite. (We work in the minimal subtraction scheme in which the counterterms contain only the singular parts necessary to make the physical quantities finite.) In practice we compute the 2-point proper vertex associated with the 1-replica part of the effective action, $\Gamma_1^{(2)}(q)$, and the 2-replica part of the effective action, Γ_2, both being evaluated for uniform configurations of the π_a fields.

The perturbative expansion is organized about the free theory formed by the quadratic part of the 1-replica action. The associated free propagators are expressed in terms of the bare quantities as follows:

$$G_{ij}(q) = T\frac{\delta_{ij} - \Pi_i\Pi_j}{q^2 + H/\Sigma}, \tag{13}$$

where $\Sigma = 1 - \mathbf{\Pi}^2$. Note that following Brezin and Zinn-Justin[28] we keep an external magnetic field H which

allows one to regularize the infrared divergences by giving a mass to the Goldstone modes. Aside from this term, the action in Eqs. (10) and (11) is $O(N)$ invariant. The loop expansion can be graphically expressed in terms of 1-particle irreducible Feynman diagrams with vertices coming from both the nonquadratic piece of the 1-replica action and from the 2-replica action.

A difficulty of the present problem lies in the functional character of the expansion, the 2-replica vertices involving the whole function $R(z)$ and its derivatives. This is somewhat similar to the treatment of disordered elastic systems,[25] with, however, the additional complication that the 1-replica part is now nontrivial and gets renormalized in a manner that couples to the renormalization of the disorder. The details of the calculation as well as the method to handle possibly anomalous terms appearing at the two-loop level when the renormalized correlator of the disorder is nonanalytic will be presented in Sec. IV.

C. FRG equations, critical exponents, and correlation functions

For the 1-replica, 2-point proper vertex and for the 2-replica effective action (when both are evaluated for uniform configurations of the fields), the relation between the renormalized and the bare theories is simply

$$\Gamma^{(2)}_{1,\mu}(q;\pi,t,h,R) = Z_\Pi \Gamma^{(2)}_{1,\mathrm{B}}(q;\mathbf{\Pi},T,H,R_0), \tag{14}$$

$$\Gamma_{2,\mu}(z,t,h,R) = \Gamma_{2,\mathrm{B}}(z,T,H,R_0), \tag{15}$$

where B denotes the bare theory.

The RG flow equations then result from the invariance of the bare theory under a change of the momentum scale μ, when T, H, and R_0 are held fixed. Actually, we are only interested in the situation of zero temperature ($T=0$) and zero external field ($H=0$). We introduce

$$\zeta_\Pi = \mu\partial_\mu \log Z_\Pi|_{R_0}, \tag{16}$$

$$\zeta_T = \mu\partial_\mu \log Z_T|_{R_0}, \tag{17}$$

and

$$\beta_R(z) = -\mu\partial_\mu R(z)|_{R_0}, \tag{18}$$

where we have implicitly set $T=H=0$. As an illustration, the flow of the 1-replica proper vertex, $t\Gamma^{(2)}_{1,\mu}(q)$, when $H=h=0$, $T=t=0$, $\mathbf{\Pi}=\pi=0$, is derived as

$$\left[\mu\partial_\mu + (2-d+\zeta_T-\zeta_\Pi) - \int_{-1}^{1} dz' \beta_R(z') \frac{\delta}{\delta R(z')}\right][t\Gamma^{(2)}_{1,\mu}(q)] = 0, \tag{19}$$

where the long-distance physics is now obtained when $\mu \to 0$.

The scaling behavior and the critical exponents of the physical quantities can be obtained from the fixed-point solutions and the properties of the flow near the fixed points. In particular, the exponents η and $\bar{\eta}$ that characterize the power-law decay of the 2-point correlation functions at the critical point for small q,

$$\overline{\langle \mathbf{S}(-\mathbf{q})\cdot\mathbf{S}(\mathbf{q})\rangle} - \overline{\langle \mathbf{S}(-\mathbf{q})\rangle\cdot\langle\mathbf{S}(\mathbf{q})\rangle} \sim q^{-(2-\eta)}, \tag{20}$$

$$\overline{\langle \mathbf{S}(-\mathbf{q})\rangle\cdot\langle \mathbf{S}(\mathbf{q})\rangle} - \overline{\langle \mathbf{S}(-\mathbf{q})\rangle}\cdot\overline{\langle\mathbf{S}(\mathbf{q})\rangle} \sim q^{-(4-\bar{\eta})}, \tag{21}$$

and the exponent θ associated with the temperature, $t=\mu^\theta T$, are given by

$$\eta = \zeta_{\Pi^*} - \zeta_{T^*}, \tag{22}$$

$$\bar{\eta} = 4 - d + \zeta_{\Pi^*}, \tag{23}$$

$$\theta = d - 2 - \zeta_{T^*} = 2 - \bar{\eta} + \eta, \tag{24}$$

where ζ_{Π^*} and ζ_{T^*} are the fixed-point values of Eqs. (16) and (17). Provided $\theta > 0$, the fixed point indeed occurs at zero renormalized temperature.

Before closing this section, it is worth recalling an inequality for the correlation functions in the present models, which turns into an inequality between critical exponents. In the RF case, the result is due to Schwartz and Soffer,[29] who have proven that the $\mathbf{q}$ Fourier component of the "connected" pair correlation function, $\overline{\langle \mathbf{S}(-\mathbf{q})\cdot\mathbf{S}(\mathbf{q})\rangle} - \overline{\langle \mathbf{S}(-\mathbf{q})\rangle\cdot\langle\mathbf{S}(\mathbf{q})\rangle}$, is always less than the square root of the $\mathbf{q}$ component of the "disconnected" pair correlation function, $\overline{\langle \mathbf{S}(-\mathbf{q})\rangle\cdot\langle\mathbf{S}(\mathbf{q})\rangle} - \overline{\langle \mathbf{S}(-\mathbf{q})\rangle}\cdot\overline{\langle\mathbf{S}(\mathbf{q})\rangle}$, up to an irrelevant multiplicative constant. As a consequence, one must have $\bar{\eta} \leqslant 2\eta$.

The RA case is different and has been considered by Feldman.[20] In this model indeed, the randomness couples to a composite field that is bilinear in the spin variables [see Eq. (1)]. As a consequence, the inequality now applies to the connected and disconnected correlation functions of the composite (bilinear) field. One can define new critical exponents, η_2 and $\bar{\eta}_2$, for those correlation functions,

$$\overline{\langle \mathbf{m}(-\mathbf{q})\cdot\mathbf{m}(\mathbf{q})\rangle} - \overline{\langle \mathbf{m}(-\mathbf{q})\rangle\cdot\langle\mathbf{m}(\mathbf{q})\rangle} \sim q^{-(2-\eta_2)}, \tag{25}$$

$$\overline{\langle \mathbf{m}(-\mathbf{q})\rangle\cdot\langle \mathbf{m}(\mathbf{q})\rangle} - \overline{\langle \mathbf{m}(-\mathbf{q})\rangle}\cdot\overline{\langle\mathbf{m}(\mathbf{q})\rangle} \sim q^{-(4-\bar{\eta}_2)}, \tag{26}$$

where $m^i(\mathbf{x}) = S^i(\mathbf{x})^2 - (1/N)$. The inequality between the correlation functions then imposes that $\bar{\eta}_2 \leqslant 2\eta_2$. However, the exponents η and $\bar{\eta}$ are no longer constrained by the usual Schwartz-Soffer inequality. The exponents η_2 and $\bar{\eta}_2$ are also expressable in terms of fixed-point quantities.

In the following we first analyze the FRG equations obtained at one-loop order near $d=4$.

III. ANALYSIS OF THE ONE-LOOP FRG EQUATIONS IN $d=4+\epsilon$

A. One-loop beta function in $d=4+\epsilon$

The beta function for the renormalized correlator of the disorder $R(z)$ at zero temperature has been obtained by Fisher at the one-loop level in $d=4+\epsilon$.[19] It reads

$$\beta_R(z) = -\mu\partial_\mu R(z)$$
$$= -\epsilon R(z) + C\Big(2(N-2)R(z)R'(1)$$
$$+\frac{1}{2}(N-2+z^2)R'(z)^2 - z(1-z^2)R'(z)R''(z)$$
$$+\frac{1}{2}(1-z^2)^2R''(z)^2 - (N-1)zR'(1)R'(z)$$
$$+(1-z^2)R'(1)R''(z)\Big), \quad (27)$$

where $C=1/(8\pi^2)$. The above expression is valid for both the RF and the RA models. The only difference is the additional inversion symmetry present in the latter: z goes from -1 to $+1$ in all cases, but in the RA model, $R(-z)=R(z)$.

At the same one-loop level, the critical exponents $\eta, \bar{\eta}$ and $\eta_2, \bar{\eta}_2$ defined in Eqs. (20), (21), (25), and (26) are given by[19,20]

$$\eta = CR'_*(1), \quad (28)$$

$$\bar{\eta} = -\epsilon + (N-1)CR'_*(1), \quad (29)$$

$$\eta_2 = (N+2)CR'_*(1), \quad (30)$$

$$\bar{\eta}_2 = -\epsilon + 2NCR'_*(1), \quad (31)$$

where the star indicates a fixed-point solution.

For studying the fixed points and their stability it is convenient to introduce $\tilde{R}(z)=(C/\epsilon)R(z)$ (the renormalized disorder is of order ϵ at the putative fixed points) and to consider the beta function for its derivative,

$$\epsilon^{-1}\beta_{\tilde{R}'}(z) = -\tilde{R}'(z) + z\tilde{R}'(z)^2 + (N-3)\tilde{R}'(z)\tilde{R}'(1)$$
$$+(N-3+4z^2)\tilde{R}'(z)\tilde{R}''(z) - (N+1)z\tilde{R}'(1)\tilde{R}''(z)$$
$$-z(1-z^2)\tilde{R}'(z)\tilde{R}'''(z) + (1-z^2)\tilde{R}'(1)\tilde{R}'''(z)$$
$$-3z(1-z^2)\tilde{R}''(z)^2 + (1-z^2)^2\tilde{R}''(z)\tilde{R}'''(z). \quad (32)$$

It is illustrative to write down the one-loop beta functions for the first derivatives $\tilde{R}'(z=1)$ and $\tilde{R}''(z=1)$, assuming that $\tilde{R}(z)$ is at least twice continuously differentiable around $z=1$. ($z=1$ corresponds to the situation where the spins in the two considered replicas become equal, $\mathbf{S}_a=\mathbf{S}_b$.) The expressions are

$$\epsilon^{-1}\beta_{\tilde{R}'(1)} = -\tilde{R}'(1) + (N-2)\tilde{R}'(1)^2, \quad (33)$$

$$\epsilon^{-1}\beta_{\tilde{R}''(1)} = -[-1+6\tilde{R}'(1)]\tilde{R}''(1) + (N+7)\tilde{R}''(1)^2 + \tilde{R}'(1)^2. \quad (34)$$

If $\tilde{R}(z)$ is analytic around $z=1$, the beta functions for the higher derivatives evaluated at $z=1$ can be derived as well. As noted by Fisher,[19] the expression for the pth derivative only involves derivatives of lower or equal order (and for $p\geqslant 3$ the beta function is linear in the pth derivative). This structure allows an iterative solution of the fixed-point equation, provided of course that $\tilde{R}(z)$ has the required analytic property.

The fixed points corresponding to the zeros of Eq. (33) are $\tilde{R}'_*(1)=0$ (stable) and $\tilde{R}'_*(1)=1/(N-2)$ (unstable with an eigenvalue $\Lambda_1=\epsilon$). The latter fixed point leads to the dimensional-reduction value of the critical exponents, e.g., $\eta=\bar{\eta}=\epsilon/(N-2)$, $\nu=1/\Lambda_1=1/\epsilon$. The second expression, Eq. (34), has then (two) nontrivial zeros only if $N\geqslant 18$: the fixed point with $\tilde{R}''_*(1)=\frac{(N-8)+\sqrt{(N-2)(N-18)}}{2(N-2)(N+7)}$ is unstable $\left(\Lambda_2=\sqrt{\frac{(N-18)}{(N-2)}}\epsilon\right)$ whereas that with $\tilde{R}''_*(1)=\frac{(N-8)-\sqrt{(N-2)(N-18)}}{2(N-2)(N+7)}$ has a negative second eigenvalue, $\Lambda_2=-\sqrt{\frac{(N-18)}{(N-2)}}\epsilon$.

This little exercise already shows that no nontrivial fixed-point function $\tilde{R}_*(z)$, twice differentiable in $z=1$, can exist for $N<18$. Actually, one finds that there is a finite range of initial conditions for $\tilde{R}'(1)$ for which, no matter what one chooses for its initial value, the RG flow for $\tilde{R}''(1)$ leads to a divergence at a *finite* scale μ. The solution to this problem has been known for some time:[23] the proper fixed point controlling the critical behavior must be nonanalytic around $z=1$, with $\tilde{R}'_*(z)$ having a cusp, i.e., a term proportional to $\sqrt{1-z}$ when $z\to 1$, at least when $N<18$.

We now consider, separately and in more detail, the results for the RF$O(N)$M and the RA$O(N)$M.

B. RF $O(N)$ model

Numerical solutions of the fixed-point equation, $\beta_{\tilde{R}'}(z)=0$, have been given by Feldman[26] for $N=3$, 4, and 5 and by us for general values of N.[22] Some analytical results can also be derived and will be discussed at the end of this section. The picture one gets from the numerical solutions is that the long-distance physics of the RF $O(N)$ model near $d=4$ drastically depends on whether N is above or below two distinct critical values: $N_{DR}=18$ and $N_c=2.8347\ldots$.

The value $N_{DR}=18$ separates a region in which $\tilde{R}'_*(z)$ at the critical, i.e., once unstable, fixed point has a cusp ($N<N_{DR}$) from a region ($N>N_{DR}$) where $\tilde{R}'_*(z)$ has only a weaker nonanalyticity, a "subcusp" in $(1-z)^{\alpha(N)}$ with $\alpha(N)$ a noninteger strictly larger than 1.[32] As already mentioned, the occurrence of a cusp changes the values of η and $\bar{\eta}$ from their dimensional-reduction value, $\eta_{DR}=\bar{\eta}_{DR}=\epsilon/(N-2)$. On the contrary, the weaker nonanalyticity occurring for $N>18$ does not alter the fixed-point value of $\tilde{R}'_*(1)$ from that obtained from Eq. (33); this leads to $\eta=\bar{\eta}=\eta_{DR}$. This is illustrated in Fig. 2 where we plot η_{DR}/η and $\bar{\eta}_{DR}/\bar{\eta}$ as a function of N.

On the contrary, at $N_c=2.8347\ldots$, the perturbative "cuspy" fixed point describing the paramagnetic-to-ferromagnetic critical point when $\epsilon>0$ disappears (η and $\bar{\eta}$ diverge as $N\to N_c^+$, see Fig. 2). Below N_c an attractive cuspy fixed point appears for $\epsilon<0$ that now describes a whole phase with QLRO. The exponents η and $\bar{\eta}$ characterizing this QLRO phase are plotted versus N in Fig. 3.

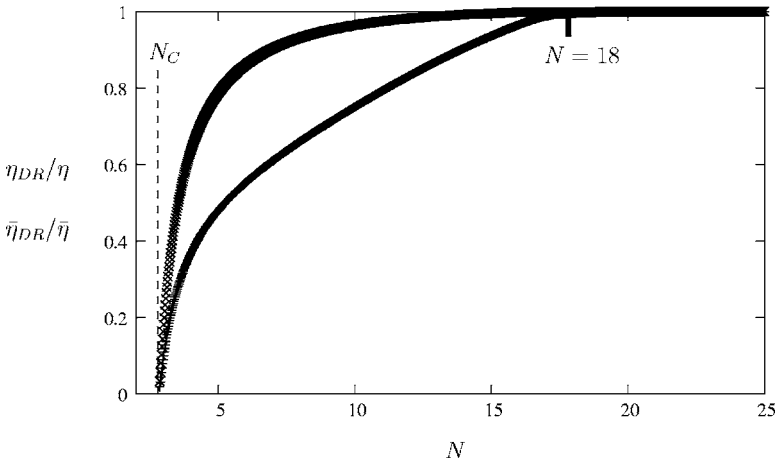

FIG. 2. Ratios η_{DR}/η (upper curve) and $\bar{\eta}_{DR}/\bar{\eta}$ (lower curve) vs N for the RF$O(N>2)M$ at first order in $\epsilon=d-4$ [the dimensional-reduction value for the exponents is $\eta_{DR}=\bar{\eta}_{DR}=\epsilon/(N-2)$]. The critical value of N at which both η and $\bar{\eta}$ diverge is $N_c=2.8347\ldots$.

At the critical value N_c, the beta function for $R'(z)$ (unscaled by ϵ) in exactly $d=4$ has a (cuspy) fixed-point solution $R'_*(z)$ for any arbitrary value of the renormalized disorder strength $R'_*(1)$. We have noted in Ref. 21 that the situation bears some similarity with the pure $O(N)$ model near $d=2$. There, the critical value N_c below which a QLRO phase may occur for $\epsilon<0$ is $N_c=2$, and for $N_c=2$ and $d=2$ the beta function for the temperature identically vanishes, independently of the value of the temperature. The singular point ($N_c=2$, $d=2$) is characterized by the existence of a Kosterlitz-Thouless transition. One may then wonder whether the singular point of the RF$O(N)$M ($N_c=2.8347\ldots$, $d=4$), despite the absence of the Abelian property specific to the $O(N=2)$ model, also possesses a Kosterlitz-Thouless transition. This point will be addressed below with the help of the two-loop calculation.

We now complement this numerical study by providing some analytical results. We first show that for $d>4$, the critical point is always characterized by a correlation-length exponent ν which is equal (at one loop) to its dimensional-reduction value, $\nu_{DR}=1/\epsilon$. The eigenvalue equation obtained by linearizing the beta function, Eq. (32), for a small deviation from the fixed-point solution, $\delta(z)=\tilde{R}'(z)-\tilde{R}'_*(z)$, is

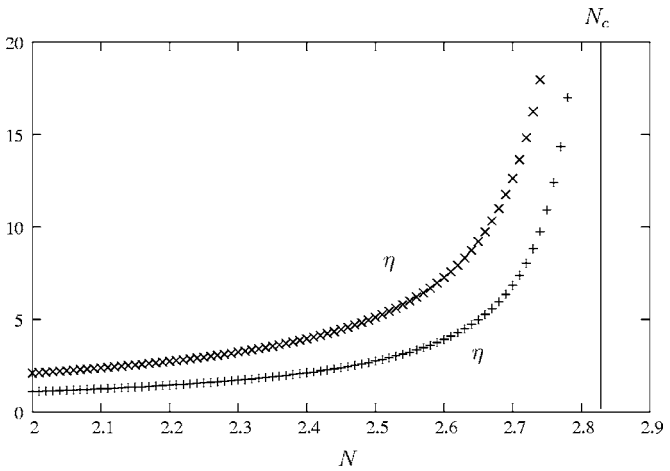

FIG. 3. Exponents η and $\bar{\eta}$ (divided by ϵ) characterizing the power-law decay of the pair correlations in the QLRO phase of the RF$O(N)$M for $N<N_c=2.8437\ldots$ (first order in $\epsilon=d-4$).

$$\frac{\Lambda}{\epsilon}\delta(z) = \delta(z)(\tilde{R}'''_*(z)z^3 + 2\tilde{R}'_*(z)z - \tilde{R}'''_*(z)z + N\tilde{R}'_*(1) - 3\tilde{R}'_*(1)$$
$$+ (4z^2 + N - 3)\tilde{R}''_*(z) - 1) + \delta(1)((N-3)\tilde{R}'_*(z)$$
$$- (N+1)z\tilde{R}''_*(z) - (z^2-1)\tilde{R}'''_*(z)) + \delta'(z)(\tilde{R}'''_*(z)z^4$$
$$- 2\tilde{R}'''_*(z)z^2 - N\tilde{R}'_*(1)z - \tilde{R}'_*(1)z + 6(z^2-1)\tilde{R}''_*(z)z$$
$$+ (4z^2 + N - 3)\tilde{R}'_*(z) + \tilde{R}'''_*(z)) - (1-z^2)$$
$$\times(z\tilde{R}'_*(z) - \tilde{R}'_*(1) - (1-z^2)\tilde{R}''_*(z))\delta''(z). \quad (35)$$

By substituting $\delta(z)=\tilde{R}'_*(z)$ in the above equation, one can easily check that the fixed-point solution is also a solution of the eigenvalue equation with a positive eigenvalue $\Lambda_1=\epsilon$ (from which $\nu=\nu_{DR}=1/\epsilon$). This result is independent of the analytic or nonanalytic character of $\tilde{R}'_*(z)$. For $d<4$, $\tilde{R}'_*(z)$ is also the solution of Eq. (35) with $\Lambda_1=\epsilon$, but the eigenvalue is now negative, which allows the fixed point to be fully attractive.

For $N>18$ it is possible to adapt Fisher's arguments concerning the hierarchy of flow equations for the successive derivatives of $\tilde{R}_*(z)$ evaluated at $z=1$.[19] (In his paper however, Fisher did not envisage nonanalytic fixed-point solutions.) As explained above, a fixed point with a well-defined second derivative and an associated negative eigenvalue ($\Lambda_2<0$) can be found for $N>18$. (Note that cuspy fixed points are also present, but they are more than once unstable and correspond to putative multicritical behavior; a detailed analysis of the fixed points and their stability in the $N\to\infty$ limit has been recently provided by Sakamoto *et al.*[27]) The flow equations for the higher derivatives are linear, namely,

$$-\mu\partial_\mu\tilde{R}^{(p)}(1) = -\Lambda_p(\tilde{R}(1),\tilde{R}(1))\tilde{R}^{(p)}(1)$$
$$+ \mathcal{F}_p(\tilde{R}(1),\tilde{R}(1),\ldots,\tilde{R}^{(p-1)}(1)), \quad (36)$$

provided of course that the pth derivative is well-defined in $z=1$. If $\tilde{R}'(1)$ and $\tilde{R}''(1)$ are chosen equal to their fixed-point values, $\tilde{R}'_*(1)=1/(N-2)$ and $\tilde{R}''_*(1)=\frac{(N-8)-\sqrt{(N-2)(N-18)}}{2(N-2)(N+7)}$, one finds

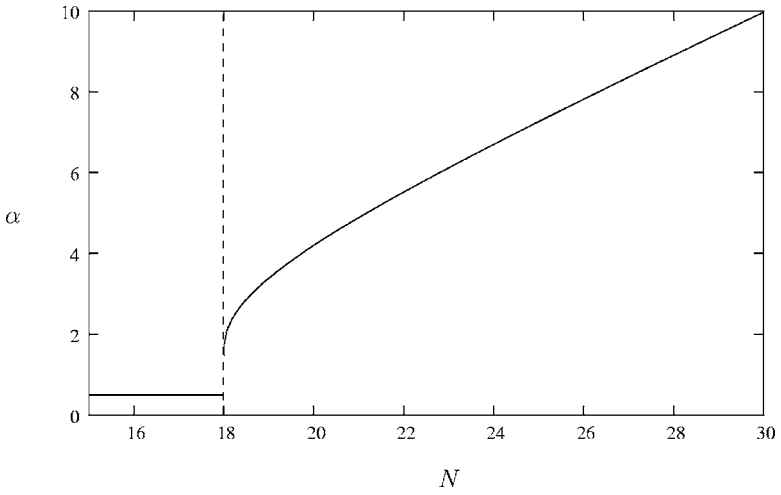

FIG. 4. Exponent $\alpha(N)$ characterizing the nonanalyticity $(1-z)^{\alpha(N)}$ in $R'(z)$ for the RF$O(N)$M in $d=4+\epsilon$ (at one loop). For $N<18$ $\alpha=1/2$ whereas $\alpha(N\to 18^{+})=3/2$.

$$\Lambda_{p^*} = \frac{\epsilon}{N-2}\left[2p^2-(N-1)p+(N-2) + \frac{p(N-5+6p)}{2(N+7)}(N-8-\sqrt{(N-2)(N-18)})\right]. \tag{37}$$

For a given N, Λ_{p^*} monotonically increases with p, so that there exists an integer value $p_{\#}(N)$ such that $\Lambda_{p_{\#}(N)^*}<0$ and $\Lambda_{p_{\#}(N)+1^*}>0$. Starting with an analytic bare action, a fixed point value is reached [provided $\tilde{R}'(1)$ is appropriately tuned] at which the first $p_{\#}(N)$ derivatives of $\tilde{R}_*(z)$ are well-defined in $z=1$. The RG flow for the $[p_{\#}(N)+1]$th derivative on the other hand goes to infinity, but only in the limit $\mu\to 0$. [This is to be contrasted with the situation for $N<18$ in which the second derivative $\tilde{R}''(1)$ diverges at a finite scale μ, due to the nonlinear nature of the corresponding beta function.] As a consequence, the $[p_{\#}(N)+1]$th derivative of $\tilde{R}_*(z)$ is not defined in $z=1$, and there must be a nonanalyticity in $\tilde{R}'_*(z)$ of the form $(1-z)^{\alpha(N)}$ with $p_{\#}(N)-1<\alpha(N)<p_{\#}(N)$.

It is easy to show that the beta function for the coefficient, say a, of the $(1-z)^{\alpha(N)}$ term is equal to $\beta_a=\Lambda_{\alpha(N)+1^*}a$, where $\Lambda_{\alpha(N)+1^*}$ is given by Eq. (37) with p replaced by the noninteger $\alpha(N)+1$. The beta function is equal to zero with a nontrivial $a\neq 0$ if and only if $\Lambda_{\alpha(N)+1^*}=0$. This selects the form of the nonanalyticity of the fixed-point solution around $z=1$. As noticed in our previous work,[22] the nonanalyticity goes as $N/2+O(1)$ at large N (a behavior that cannot be captured in a $1/N$ expansion, see, e.g., Ref. 27). However, contrary to what is stated in Ref. 22, the exponent of the subcusp increases continuously with N when $N>18$, as illustrated in Fig. 4.

Finally, we close this survey of the RF$O(N)$M at one-loop order by pointing out that for $N=2$, the FRG equations, Eqs. (27)–(29), exactly reduce to those of a periodic elastic system, with a one-component displacement field, pinned by disorder. This is more easily seen by switching variables from z to an angle $\phi=\cos^{-1}(z)$. A cuspy fixed-point solution [with $\eta=|\epsilon|\pi^2/9$ and $\bar{\eta}=|\epsilon|(1+\pi^2/9)$] describing a QLRO phase (a "Bragg glass") when $d<4$ is then analytically obtained (compare with Refs. 8, 9, and 5).

C. RA $O(N)$ model

Overall, the picture of the long-distance physics of the RA $O(N)$ model that one gets from solving the one-loop FRG equations is very similar to that of the RF $O(N)$ model. This conclusion, we recall, comes with the proviso that one focuses on weak disorder (working near the lower critical dimension of the paramagnetic-to-ferromagnetic transition) and that the possible spin-glass ordering which may occur at stronger (finite) disorder is not considered. The main difference with the behavior of the RF $O(N)$ model then lies in the critical values N_{DR} and N_c: N_c is found to be 9.4412…; on the other hand, $N_{DR}=\infty$, which means that, contrary to the RF case, a cusp appears for all values of N and dimensional reduction always breaks down completely.

To show that the fixed-point solution $\tilde{R}'_*(z)$ always has a cusp, it is instructive to go back to the beta functions for the first two derivatives $\tilde{R}'(1)$ and $\tilde{R}''(1)$, Eqs. (33) and (34), assuming that there is no cusp, $(1-z)^{\alpha}$ with $0<\alpha<1$, in $\tilde{R}'(z)$. The RA model having the additional inversion symmetry, $\tilde{R}(-z)=\tilde{R}(z)$, it is convenient to rewrite $\tilde{R}(z)=(1/2)\tilde{S}(z^2)$. From Eqs. (33) and (34) one obtains the flow equations for $\tilde{S}'(1)$ and $\tilde{S}''(1)$. A nontrivial fixed point of the beta function for $\tilde{S}'(1)=\tilde{R}'(1)$ is again $\tilde{R}'_*(1)=1/(N-2)$ and the associated eigenvalue is positive $(\Lambda_1=\epsilon)$, so that the fixed point can only be reached if one tunes the initial value to be exactly $1/(N-2)$. When doing so, the flow equation for $\tilde{S}''(1)$ can now be written as

$$-\epsilon^{-1}\mu\partial_\mu\tilde{S}''(1)=\frac{1}{2(N-2)^2}+2(N+7)[\tilde{S}''(1)-\tilde{S}''_+]\times[\tilde{S}''(1)-\tilde{S}''_-], \tag{38}$$

where

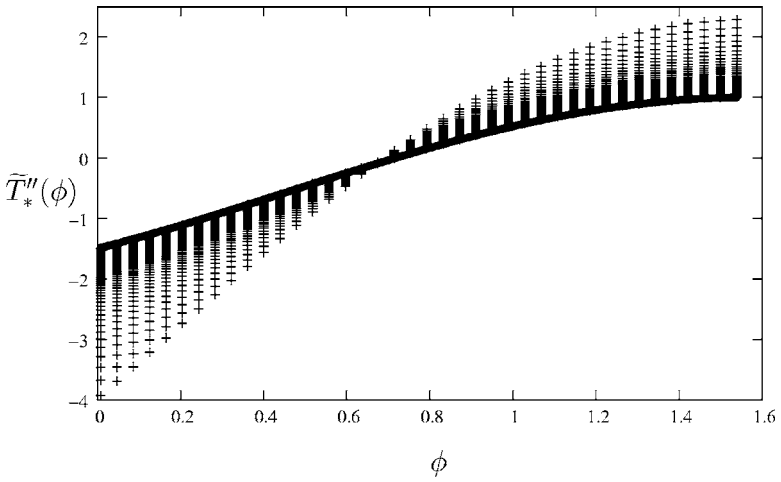

FIG. 5. Variation with N of the (cuspy) fixed point of the RA$O(N)$M in $d=4+\epsilon$ (at one loop): $\tilde{T}''_*(\phi)$ vs ϕ for $0 \leqslant \phi \leqslant \pi/2$. The curves correspond to $N=16$ (top curve in the right part of the figure) and to $N=1500$ (bottom curve in the right part of the figure) by steps of 5% relative increase. The thick curve is the analytical result for $N \to \infty$ [see Eq. (41)]. Note that there is a zero slope when $\phi=\pi/2$ and a nonzero one (i.e., a cusp) when $\phi \to 0^+$.

$$\tilde{S}''_{\pm} = -\left[\frac{(N+22) \mp \sqrt{(N-2)(N-18)}}{2(N-2)(N+7)}\right]$$

are both strictly negative for any finite value of N. If one starts with a value of $\tilde{S}''(1)$ that is positive or even zero, which is indeed a physical requirement since the bare disorder correlator is of the form $\tilde{\Delta}_2 z^2$ plus possible higher-order even powers of z associated with even-rank anisotropies, the beta function, i.e., the right-hand side of Eq. (38), stays strictly positive. As a result, $\tilde{S}''(1)$ diverges, and it actually diverges at a finite scale μ. This is of course incompatible with the hypothesis that the fixed point has a well-defined second derivative $\tilde{S}''_*(1)$: a cusp must appear along the flow. Note that this reasoning is completely independent of N.

The limit $N \to \infty$ is, however, somewhat special. Looking for $\tilde{S}(z^2)=O(1/N)$ and taking the $N \to \infty$ limit in Eq. (38), one finds

$$-\epsilon^{-1}\mu\partial_\mu(N\tilde{S}''(1))_\infty = 2(N\tilde{S}''(1))_\infty[(N\tilde{S}''(1))_\infty + 1]. \quad (39)$$

A fixed point with $\tilde{S}''_*(1)=0$, although having a second positive eigenvalue, can still be reached from an initial condition with $\tilde{S}''(1)=0$: this analytic fixed point is the one found by a direct analysis of the $N \to \infty$ saddle-point equation of an RA model with *only* a second-rank anisotropy, $\Delta_2 z^2$. It is, however, unstable to the introduction of higher-order anisotropies (and of course never stable when N is large but finite).

One can actually find the cuspy fixed-point solution in the large N limit. It is convenient to change the variable from z to $\phi=\cos^{-1}(z)$ and define $\tilde{T}(\phi)=(N-2)\tilde{R}(z)$. $\tilde{T}(\phi)$ must be an even function of ϕ and the symmetry $\tilde{R}(-z)=\tilde{R}(z)$ translates into $\tilde{T}(\pi-\phi)=\tilde{T}(\phi)$, so that it is sufficient to consider ϕ in the interval $[0, \frac{\pi}{2}]$. The beta function for $\tilde{T}'(\phi)$ in the large N limit is given by

$$\begin{aligned}\epsilon^{-1}\beta_{\tilde{T}'}(\phi) = &-\tilde{T}'(\phi) - \frac{\cos(\phi)}{\sin^3(\phi)}\tilde{T}'(\phi)^2 \\ &+ \frac{\tilde{T}'(\phi)}{\sin^2(\phi)}[\cos(2\phi)\tilde{T}''(0) + \tilde{T}''(\phi)] \\ &- \frac{\cos(\phi)}{\sin(\phi)}\tilde{T}''(0)\tilde{T}''(\phi) + \frac{\tilde{T}'''(\phi)}{N-2}[\tilde{T}''(\phi) - \tilde{T}'(0)],\end{aligned} \quad (40)$$

where the last term can be dropped in the large N limit. Details on the derivation of the solution and on the stability analysis are provided in Appendix A. Here, we only quote the result:

$$\tilde{T}'_*(\phi) = -3\sin(\phi)\cos\left(\frac{\pi+|\phi|}{3}\right) + \mathcal{O}\left(\frac{1}{N}\right). \quad (41)$$

The $1/N$ correction can also be analytically obtained and is given in Appendix A. One can see that $\tilde{T}'_*(\phi)$ in Eq. (41) satisfies the symmetry requirement around $\frac{\pi}{2}$, since $\tilde{T}'_*(\frac{\pi}{2})=0$, and has a cusp in $|\phi|$ (i.e., in $\sqrt{1-z}$) as ϕ goes to zero (and z goes to 1). The fixed point is once unstable with, as shown in the previous section, $\Lambda_1=\epsilon$; hence $\nu=\nu_{DR}=1/\epsilon$. The critical exponents $\eta, \bar{\eta}$ and $\eta_2, \bar{\eta}_2$ are obtained from $\tilde{R}'_*(1)=-\tilde{T}''_*(0)/(N-2)=\frac{3}{2N}+\frac{26}{N^2}+O(1/N^3)$ [see Eqs. (28)–(31)]:

$$\eta = \frac{3\epsilon}{2N}\left[1 + \frac{52}{3N} + \mathcal{O}\left(\frac{1}{N^2}\right)\right], \quad (42)$$

$$\bar{\eta} = \frac{\epsilon}{2}\left[1 + \frac{49}{N} + \mathcal{O}\left(\frac{1}{N^2}\right)\right], \quad (43)$$

$$\eta_2 = \frac{3\epsilon}{2}\left[1 + \frac{58}{3N} + \mathcal{O}\left(\frac{1}{N^2}\right)\right], \quad (44)$$

$$\bar{\eta}_2 = 2\epsilon\left[1 + \frac{26}{N} + \mathcal{O}\left(\frac{1}{N^2}\right)\right]. \quad (45)$$

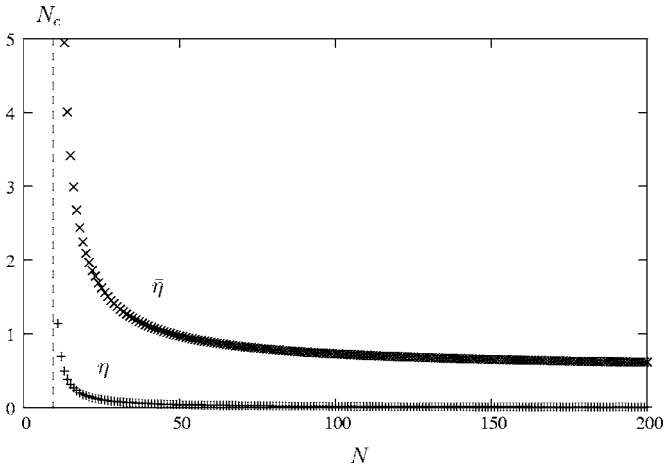

FIG. 6. Exponents η and $\bar{\eta}$ (divided by ϵ) for the RA$O(N)$M at first order in $\epsilon=d-4$. Dimensional reduction fails for all values of N: $\epsilon^{-1}\eta \sim 3/(2N)$ and $\epsilon^{-1}\bar{\eta} \sim 1/2$ when $N \to \infty$. The critical value of N at which both η and $\bar{\eta}$ diverge is $N_c=9.4412\ldots$.

Note that a Schwartz-Soffer-like inequality is satisfied, as it should be (see Sec. III A), by the exponents η_2 and $\bar{\eta}_2$ (namely, $\bar{\eta}_2 < 2\eta_2$), but *not* by the exponents η and $\bar{\eta}$.

We display in Fig. 5 the large N cuspy fixed-point solution, Eq. (41), together with the numerical solution obtained for a wide span of N. The convergence to the $N \to \infty$ limit is clearly visible, as is visible the presence for all N's of a nonzero slope as $\phi \to 0$, which corresponds to a cusp. In Fig. 6 we display the exponents η and $\bar{\eta}$ as a function of N; this again illustrates that dimensional reduction fails for all values of N.

The change from ferromagnetic ordering to QLRO occurs for $N_c=9.441\ldots$, to be compared to $N_c=2.834\ldots$ for the RF$O(N)$M. As first shown by Feldman,[20] QLRO may thus be present in the RA$O(N)$M near, but below, $d=4$ for $N=2,3,\ldots,9$: see also Fig. 7. The (cuspy) fixed-point solution associated with QLRO can be analytically derived in the $N=2(XY)$ case. Just like in the RF$O(N)$M, the FRG equations

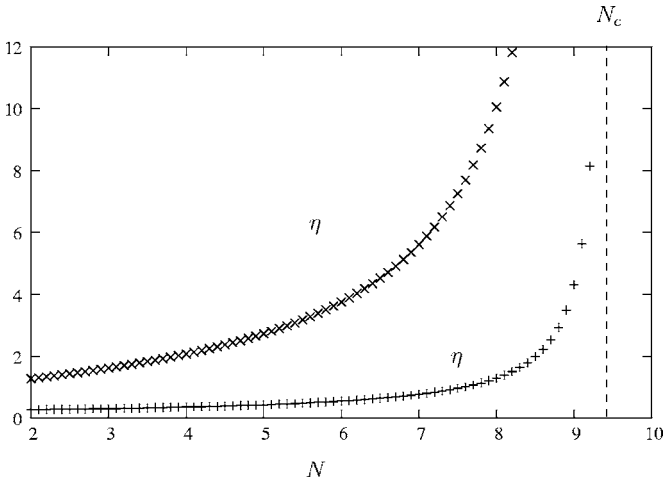

FIG. 7. Exponents η and $\bar{\eta}$ (divided by ϵ) characterizing the power-law decay of the pair correlations in the QLRO phase of the RA$O(N)$M for $N < N_c=9.4412\ldots$ (first order in $\epsilon=d-4$).

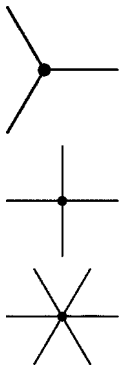

FIG. 8. Vertices with three and four legs obtained from $\mathcal{S}_1$, i.e., with one replica.

then reduce to those of a disordered periodic elastic system,[5,8,9] the only difference with the RF case being a simple rescaling of the solution accounting for the difference in the periodicity, from 2π to π. This yields the critical exponents $\eta=|\epsilon|\pi^2/36$ and $\bar{\eta}=|\epsilon|(1+\pi^2/36)$.

IV. DERIVATION OF THE FRG BETA FUNCTIONS TO TWO LOOPS

In this section we describe in detail the calculation of the beta functions and of the critical exponents at two loops.

A. Diagrammatic representation

As explained above (see Sec. II B) the calculation is based on an expansion of the effective action in powers of R. The terms of this expansion are given by all amputated 1-particle irreducible Feynman diagrams. In order to determine all the counterterms, we need to compute the 1-replica 2-point proper vertex and the 2-replica effective action with no derivatives (uniform fields). The associated diagrams are obtained by connecting the different vertices of the theory with the free propagator given in Eq. (13).

The free propagator is represented by a line. The vertices are obtained by deriving either $\mathcal{S}_1$ [Eq. (10)] or $\mathcal{S}_2$ [Eq. (11)]. In the former case they are represented by lines emerging from a single circle (see Fig. 8) and in the latter by lines emerging from two circles (corresponding to the two replicas of $\mathcal{S}_2$) connected by a dashed line (see Fig. 9).

As can be seen in Eqs. (8) and (9) the 1- and 2-replica parts of the action have a factor T^{-1} and T^{-2}, respectively, so that the various diagrams do not come with the same power of the temperature. Anticipating that the fixed point of interest to us is at zero temperature, we compute here only the diagrams of lowest order in T, i.e., those proportional to $1/T$ for the 1-replica effective action and to $1/T^2$ for the 2-replica effective action. It is easy to check that the diagrams of lowest order in temperature with n_1 1-replica vertices and n_2 2-replica vertices have n_1+2n_2-2 propagators. Similarly, for the 2-replica effective action, the diagrams of lowest order in temperature have n_1+2n_2-1 propagators. Given these constraints, one can draw all the diagrams and check that an expansion in powers of R corresponds to an expansion in

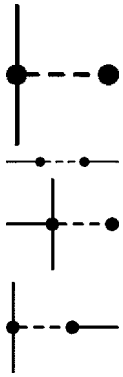

FIG. 9. Vertices with two and three legs obtained from $\mathcal{S}_2$, i.e., with two replicas.

increasing number of loops. The one-loop diagrams are displayed in Figs. 10 and 11.

The two-loop diagrams are given in Appendix B. The integrals involved in the two-loop calculations have been evaluated in the dimensional regularization scheme by using the procedure described in Appendix C.

The 1-replica 2-point proper vertex can be formally expressed as

$$\frac{\delta^2\Gamma_1[\pi]}{\delta\pi^i(q)\delta\pi^j(q)} = Z_\Pi\left[\frac{1}{T}\left(q^2 - \frac{H}{\Sigma}\right)\left(\delta_{ij} + \frac{\Pi_i\Pi_j}{\Sigma^2}\right) + \text{one-loop} + \text{two-loops}\right] \tag{46}$$

with $\Sigma = 1 - \mathbf{\Pi}^2$. The first term in the parentheses corresponds to the tree diagram and is given by the inverse of the free propagator [see Eq. (13)].

The same can be done for the 2-replica effective action, which formally gives

$$\Gamma_2[\mathbf{\Pi}_a, \mathbf{\Pi}_b] = \frac{1}{T^2}R_0(\mathbf{\Pi}_a \cdot \mathbf{\Pi}_b + \Sigma_a\Sigma_b) + \text{one-loop} + \text{two-loops}. \tag{47}$$

We next replace the bare quantities by the renormalized ones, following Eqs. (12), in the two previous expressions and reexpand in powers of R. One must then choose the counterterms such that the expressions are finite, i.e., such that all terms in $1/\epsilon$ and $1/\epsilon^2$ vanish.[33]

Once the counterterms are known, the beta functions can be calculated as derivatives of the renormalized quantities with respect to the scale μ at fixed bare quantities [see Eqs. (16)–(18)]. In order to perform the derivative in Eq. (18), we write the counterterm for R as

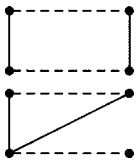

FIG. 10. One-loop diagrams for the 2-replica effective action.

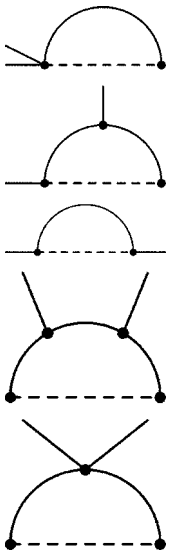

FIG. 11. One-loop diagrams for the 1-replica 2-point proper vertex.

$$Z_R = R + \delta_1[R,R] + \delta_2[R,R,R], \tag{48}$$

where $\delta_1[R,R]$ and $\delta_2[R,R,R]$ are the one-loop and two-loop contributions, respectively; the former is a quadratic functional of R and is proportional to $1/\epsilon$, and the latter is cubic in R and contains terms in $1/\epsilon^2$ and $1/\epsilon$. We then invert Eq. (12d) with Z_R given by Eq. (48), so that the renormalized function R can be expressed as a functional of the bare function R_0 as

$$R = \mu^\epsilon R_0 - \mu^{2\epsilon}\delta_1[R_0,R_0] - \mu^{3\epsilon}(\delta_2[R_0,R_0,R_0] - 2\delta_1[\delta_1[R_0,R_0],R_0]) + O(R_0^4). \tag{49}$$

The term on the last line corresponds to a repeated one-loop term, in which the first argument of the functional δ_1 is replaced by $\delta_1[R_0,R_0]$. This gives a cubic contribution in R_0. The flow equation for R is then given by Eq. (18) with the following beta function:

$$\beta_R = -\epsilon(R - \delta_1[R,R] - 2\delta_2[R,R,R] + 2\delta_1[\delta_1[R,R],R]). \tag{50}$$

In the above expression, the terms in $1/\epsilon$ appearing in δ_1, δ_2, and in the repeated one-loop term are multiplied by ϵ and therefore give finite contributions. The last two terms also have contributions in $1/\epsilon^2$, but they exactly cancel each other [as can be explicitly checked by using Eqs. (53) and (54) below].

B. Analytic piece of the beta functions

As discussed in Sec. III, even when starting from an analytic initial condition, integration of the one-loop flow equation generates a nonanalyticity in the renormalized disorder function $R(z)$. It is therefore necessary to consider the flow equations for nonanalytic functions $R(z)$, and in particular to determine the contributions of such nonanalyticities to the beta functions. At the one-loop order, there are no such contributions. However, they appear at two loops. For clarity's sake, we first describe the calculation of the flow equations

for analytic functions and consider the contributions due to nonanaliticities in the next section.

The analysis described in the previous section and in Appendixes B and C leads to the following expressions for the counterterms:

$$Z_{\Pi}^{\mathrm{r}} = 1 + \frac{C}{\epsilon}(N-1)R'(1)\left(1 + \frac{C}{2\epsilon}R'(1)(2N-3)\right), \quad (51)$$

$$Z_{T}^{\mathrm{r}} = 1 + \frac{C}{\epsilon}(N-2)R'(1)\left(1 + \frac{C}{\epsilon}R'(1)\left(N-2+\frac{\epsilon}{2}\right)\right), \quad (52)$$

$$\frac{2\epsilon}{C}\delta_1[R,R] = (z^2+N-2)R'(z)^2 + 2z((1-N)R'(1) + (z^2-1)R''(z))R'(z) + 4(N-2)R(z)R'(1) + (z^2-1)R''(z)((z^2-1)R''(z) - 2R'(1)), \quad (53)$$

$$\frac{4\epsilon^2}{C^2}\delta_2^{\mathrm{r}}[R,R,R] = (\epsilon+2)R''(z)R'''(z)^2(z^2-1)^4 + 2R''(z)^2[3z(\epsilon+4)R'''(z) + (z^2-1)R''''(z)](z^2-1)^3 + [(9\epsilon+32)z^2 + N(\epsilon+2) - 2(\epsilon+6)]R''(z)^3(z^2-1)^2 + R'(z)[z[15(\epsilon+4)z^2 + N(3\epsilon+10) - 2(6\epsilon+25)]R''(z)^2 + 2(z^2-1)([4(\epsilon+5)z^2 + 2N - \epsilon - 6]R'''(z) + 2z(z^2-1)R''''(z))R''(z) + z(z^2-1)^2(\epsilon+2)R'''(z)^2](z^2-1) + z[(\epsilon+4)z^2 + 2N - \epsilon - 6]R'(z)^3 + 4(N-2)(3N+\epsilon-6)R(z)R'(1)^2 + 2R'(1)^2\{(-4N^2+13N-9)zR'(z) + [N^2z^2 + 9z^2 - 3N(z^2-1) - 10] \times R''(z) + (z^2-1)[2(N+1)zR'''(z) + (z^2-1)R''''(z)]\} + R'(z)^2([(7\epsilon+32)z^4 - 12(\epsilon+4)z^2 + 2N^2 + 5\epsilon + 2N(z^2-1)(\epsilon+5) + 14]R''(z) + 2z(z^2-1)\{[(\epsilon+8)z^2 + 2N - \epsilon - 6]R'''(z) + z(z^2-1)R''''(z)\}) - R'(1)[(\epsilon+2)R'''(z)^2(z^2-1)^3 + 2R''(z)[z(2N+3\epsilon+14)R'''(z) + 2(z^2-1)R''''(z)](z^2-1)^2 + \{(7\epsilon+34)z^2 - 4(\epsilon+6) + N[(\epsilon+6)z^2 + 2(\epsilon+2)]\}R''(z)^2(z^2-1) + \{-4N^2 + [(\epsilon-2)z^2 - \epsilon + 18]N - z^2(\epsilon-10) + \epsilon - 22\}R'(z)^2 + 2R'(z)(z[2N^2 + (z^2-1)(\epsilon+2)N - \epsilon + z^2(\epsilon+18) - 20]R''(z) + (z^2-1)\{[(\epsilon+10)z^2 + 2N(z^2+1) - \epsilon - 6]R'''(z) + 2z(z^2-1)R''''(z)\})], \quad (54)$$

where the superscript r stands for "regular" (i.e., analytic), $C^{-1}=8\pi^2$ and $z=\pi_a\cdot\pi_b+\sqrt{1-\pi_a^2}\sqrt{1-\pi_b^2}$.

Note that the expressions for Z_{Π} and Z_T correspond to those obtained at two loops in the nonlinear sigma model for the ferromagnetic-paramagnetic transition of the $O(N)$ model with no randomness if one replaces $R'(1)$ by the temperature, C by $1/2\pi$, and ϵ by $d-2$.[28] Moreover, the counterterm for $R'(1)$ [assuming here that the function $R(z)$ is analytic] reads

$$\frac{1}{R'(1)}\partial_z(\delta_1+\delta_2^{\mathrm{r}})|_{z=1} = \frac{C}{\epsilon}R'(1)(N-2)\left[1 + \frac{C}{\epsilon}R'(1)\left(N-2+\frac{\epsilon}{2}\right)\right], \quad (55)$$

which again coincides with the counterterm found for the temperature in the pure system.[28] This equivalence between the pure model near $d=2$ and the disordered one near $d=4$ is the expression of the dimensional-reduction property.

The regular part of the beta function for $R(z)$ can then be calculated from Eqs. (50), (53), and (54), which gives

$$\beta_R^{\mathrm{r}}(z) = -\epsilon R(z) + \frac{C}{2}\{(N-2+z^2)R'(z)^2 - 2z[(1-z^2)R''(z) + (N-1)R'(1)]R'(z) + 4(N-2)R(z)R'(1) + (1-z^2)R''(z)[(1-z^2)R''(z) + 2R'(1)]\} + \frac{C^2}{2}\{(1-z^2) \times [(1-z^2)R''(z) + R'(1) - zR'(z)][(1-z^2)R'''(z) - 3zR''(z) - R'(z)]^2 + (N-2)[(1-z^2)^2R''(z)^3 - (1-z^2)[3zR'(z) - (z^2+2)R'(1)]R''(z)^2 - 2(1-z^2)R'(z)[R'(z) - zR'(1)]R''(z) + (1-z^2)R'(1)R'(z)^2 + 4R(z)R'(1)^2]\}. \quad (56)$$

We next consider the derivation of the critical exponents. The determination of ζ_{Π} and ζ_T simplifies if one uses the fact that Z_{Π} and Z_T depend on $R(z)$ only through $R'(1)$. Equations (16) and (17) become

$$\zeta_A^{\mathrm{r}} = \mu\partial_\mu \log Z_A^{\mathrm{r}} = -\beta_{R'(1)}\partial_{R'(1)} \log Z_A^{\mathrm{r}} \quad (57)$$

with A being Π or T and the derivatives being taken at fixed bare quantities. We then get

$$\zeta_{\mathrm{II}}^{r} = (N-1)CR'(1) + \mathcal{O}(R^3), \tag{58}$$

$$\zeta_{T}^{r} = (N-2)CR'(1)[1 + CR'(1)] + \mathcal{O}(R^3). \tag{59}$$

The critical exponents η and $\bar{\eta}$ can now be evaluated by making use of Eqs. (22) and (23):

$$\eta^{r} = CR_*(1)[1 - (N-2)CR_*(1)], \tag{60}$$

$$\bar{\eta}^{r} = -\epsilon + (N-1)CR_*(1). \tag{61}$$

As we shall explicitly show in Sec. V, the exponents defined under the assumption of an analytic fixed-point solution $R_*(z)$ are equal to their dimensional-reduction value.

C. "Anomalous" contributions

We have seen in Sec. III that, even with an analytic initial condition for $R_{t=0}(z)$, the one-loop RG flow equation generates a nonanalyticity in the renormalized disorder function $R(z)$. The strongest nonanalyticity is obtained in the RF$O(N)$M for $N<18$ and in the RA$O(N)$M for all values of N in the form

$$R(z) = R(1) + R'(1)(z-1) - \frac{a}{3}[2(1-z)]^{3/2} + \ldots \tag{62}$$

when z approaches 1 (from below); a will be used in the following to quantify the strength of the singularity. Dimensional reduction is recovered under the assumption that the function $R(z)$ is analytic (see above), but if $a \neq 0$ it is no longer valid.

Alternatively, the renormalized disorder function can be parametrized in terms of the angle ϕ between the two replicas instead of the scalar product z ($z=\cos\phi$). The expansion in Eq. (62) then translates into a small ϕ expansion,

$$R(\phi) \equiv R(z=\cos\phi) = R(1) - R'(1)\frac{\phi^2}{2} - \frac{a|\phi|^3}{3} + \ldots, \tag{63}$$

where the nonanalyticity appears as a discontinuity in the third derivative of $R(\phi)$ in $\phi=0$.

One can easily convince oneself that the nonanalytic term in a can explicitly appear in $\beta_R(z)$. Consider the repeated one-loop term [last term in Eq. (50)]. Since $\delta_1[R,R]$ has an explicit dependence on $R'(1)$, one has to compute $\partial_z \delta_1|_{z=1}$ which, when the nonanalyticity of $R(z)$ is taken into account [see Eq. (62)], takes the form

$$\partial_z \delta_1|_{z=1} = \frac{C}{\epsilon}[R'(1)^2(N-2) - a^2(N+2)].$$

Replacing then $R'(1)$ by Eq. (62) yields an explicit dependence of β_R on a.

Actually, the two-loop, 2-replica diagrams also give contributions in a^2: look, for instance, at the sixth diagram of Fig. 14 in Appendix B. Note that the two replicas of the vertices on the left and on the right of the diagram are actually connected via propagators. These vertices are therefore to be computed for identical replicas. In order to take into account the nonanalytic part of this diagram, the 2-replica vertices are evaluated for two slightly different replicas $\mathbf{S}_a$ and $\mathbf{S}_{a'}$ with

$$\mathbf{S}_{a'} = \frac{\mathbf{S}_a + \alpha\boldsymbol{\Delta}}{\sqrt{1+\alpha^2}}. \tag{64}$$

Here, α is a small parameter that must be taken to zero at the end of the calculation and $\boldsymbol{\Delta}$ is a unit vector orthogonal to $\mathbf{S}_a$ that gives the direction in which $\mathbf{S}_{a'}$ approaches $\mathbf{S}_a$. The dependence of the diagram on $\boldsymbol{\Delta}$ appears only through the scalar product $\boldsymbol{\Delta}\cdot\mathbf{S}_b$ whose absolute value varies between 0 (when $\boldsymbol{\Delta}$ and $\mathbf{S}_b$ are orthogonal) and $\sqrt{1-z^2}$ (when $\boldsymbol{\Delta}$, $\mathbf{S}_a$, and $\mathbf{S}_b$ are in the same plane). We therefore write

$$\boldsymbol{\Delta}\cdot\mathbf{S}_b = \gamma\sqrt{1-z^2} \tag{65}$$

with γ varying between -1 and 1.

There are six 2-replica diagrams giving nonanalytic contributions in a^2: diagrams 5, 6, 11, 12, 13, and 14 of Fig. 14. These diagrams (and some others) also have contributions linear in a, but we discard them for symmetry reasons. Indeed, a corresponds to the third derivative of $R(\phi)$ [see Eq. (63)] which changes sign under the operation $\phi \to -\phi$. On the other hand, the disorder function itself is unchanged in the same operation; as a result, linear contributions in a must vanish from all physical quantities.

The situation is even more complex when considering the two-loop diagrams for the 1-replica 2-point function. In this case a generic diagram has a singular limit $\alpha \to 0$. Indeed an expansion in powers of α around 0 gives terms in $a^2\alpha^{-2}$, $a^2\alpha^{-1}$, and $a^2\alpha^0$. On top of this, there is a strong dependence of the result on the way the regularization is performed. Look for instance at the first diagram of Fig. 15. We can decide to attribute the field $\mathbf{S}_a$ to the replica on the left of the diagram and the field $\mathbf{S}_{a'}$ to the replica on the right. It remains to choose whether the propagator (which is diagonal in replica indices) on the top of the diagram is associated with $\mathbf{S}_a$ or $\mathbf{S}_{a'}$. The calculation shows that the two choices lead to different results.

Such ambiguities are already present in the two-loop FRG treatment of disordered elastic systems and Le Doussal, Wiese, and co-workers have given a detailed and well-argumented analysis of the way to handle these ambiguities.[25] Here, we have extended their procedure and used the following set of rules

1. The nonanalytic parts of the diagrams, i.e., those proportional to a^2, come with an *a priori* unknown weight.
2. Within a single diagram, the parts in $a^2\alpha^{-2}$, $a^2\alpha^{-1}$, and $a^2\alpha^0$ come with independent (*a priori* unknown) weights.
3. For diagrams that are ambiguous in the sense that different regularization schemes lead to different results, we have introduced additional weighting factors such that all possible results can be reproduced by appropriately choosing these extra weighting factors.

As discussed in Ref. 25, the fact that pieces of the two-loop diagrams come with *a priori* unknown weighting factors is due to the intrinsic ambiguity that occurs at $T=0$ when the function R entering into the vertices is nonanalytic in z

$=1$ (or $\phi=0$). Consider for instance the third derivative of $R(\phi)$ around $\phi=0$ [see Eq. (63)]. Its sign depends on whether $\phi\to 0^+$ or $\phi\to 0^-$ and because of the discontinuity its value in exactly $\phi=0$ is left undetermined. Vertices that contain this derivative evaluated exactly in $\phi=0$ have thus a contribution that come with an undetermined weight. Additional constraints must be used to fix the values of the weighting factors (or at least enough relations between these factors). This is precisely what is done by requiring that the physical quantities be finite.

Under these hypotheses, the calculation proceeds in a straightforward way. We observe that it is possible to choose the nonanalytic part of the counterterms and to fix all the weighting factors such that the 1-replica 2-point proper vertex and the 2-replica effective action [see Eqs. (46) and (47)] are finite. This procedure leads to a *unique* form for the counterterms [for a given parameter γ, see Eq. (65)]. On top of the analytic parts already computed [see Eqs. (51)–(54)], one now must add the "anomalous" contributions, so that

$$Z_{\Pi} = Z_{\Pi}^{\mathrm{r}} - \frac{C^2}{\epsilon^2} a^2 \left(\frac{(N-1)(N+2)}{2} + \epsilon \frac{3N-2}{4} \right), \tag{66}$$

$$Z_T = Z_T^{\mathrm{r}} - \frac{C^2}{\epsilon^2} a^2 \left(\frac{N^2-4}{2} + \epsilon \frac{N-2}{2} \right), \tag{67}$$

$$\begin{aligned} \delta_2[R,R,R] = \delta_2^{\mathrm{r}}[R,R,R] + \frac{C^2 a^2}{\epsilon^2} \Bigg\{ & [4 - N^2 - (N-2)\epsilon] R(z) \\ & + \frac{z}{4} [2(N-1)(N+2) + \epsilon(3N-2)] R'(z) \\ & - \frac{1-z^2}{4} [2N + 4 + (2+\gamma^2 N)\epsilon] R''(z) \Bigg\}. \end{aligned} \tag{68}$$

The presence of "anomalous" contributions in the counterterms induce new terms in the beta function for $R(z)$, which now reads

$$\begin{aligned} \beta_R(z) = \beta_R^{\mathrm{r}}(z) - \frac{C^2 a^2}{2} \{ & 4(N-2) R(z) - (3N-2) z R'(z) \\ & + (1-z^2)(\gamma^2 N + 2) R''(z) \}, \end{aligned} \tag{69}$$

where, we recall, a is defined through Eq. (62). Note here that there is still an explicit dependence on γ^2, which encodes how one takes the limit $\mathbf{S}_{a'} \to \mathbf{S}_a$ [see Eq. (65)]. There is, however, a preferred value for γ^2. The simplest way to see this is to compute $\beta_R(z)$ with a nonanalytic function R of the form given in Eq. (62). There is a term proportional to $a^3(1-\gamma^2)\sqrt{1-z}$. If we choose $\gamma^2 \neq 1$, the flow equation generates a *supercusp*, i.e., a stronger nonanalyticity, $R(z) \sim (1-z)^{1/2}$, than the one initially considered; this supercusp would itself generate an even stronger nonanalyticity and the theory would not be renormalizable at the two-loop level. On the other hand, $\gamma^2=1$ ensures that the procedure is consistent. The value $\gamma^2=1$ also appears in another context: the repeated one-loop term [last term of Eq. (50)] can be interpreted as the set of two-loops diagrams obtained by replacing in the one-loop diagrams (see Fig. 10) one of the 2-replica vertices by the one-loop diagrams with two external legs. If we compute these two-loop diagrams with their weighting factor according to the above procedure, we get an expression that is consistent with the repeated term only if we choose $\gamma^2=1$. In the following, we thus fix γ^2 to this value.

It is worth stressing that Eqs. (56) and (69) (with $\gamma^2=1$) exactly reduce to the two-loop FRG equation for periodic disordered elastic systems when $N=2$.[25] This is more easily checked by switching to the angle variable ϕ.

In Refs. 21 and 30 the renormalization constant for the temperature Z_T had not been derived at two loops, so that an incompletely determined version of the beta function of Eq. (69) was given. In the notations of Ref. 21 the unknown parameter K is now fixed to $K=1/2$ whereas in the notations of Ref. 30 the unknown parameter is now fixed to $\gamma_a = 1/4$.[34]

Finally, the expressions of the critical exponents have to be modified in order to take into account the nonanalytic contributions. One obtains

$$\eta = \eta^{\mathrm{r}} - \frac{C^2 a_*^2}{2} (N+2) \tag{70}$$

$$\bar{\eta} = \bar{\eta}^{\mathrm{r}} - \frac{C^2 a_*^2}{2} (3N-2), \tag{71}$$

where a_* is the fixed-point value for the parameter a.

V. DISCUSSION OF THE FIXED POINTS AT THE TWO-LOOP LEVEL AND CONCLUSION

Going from the one-loop to the two-loop order does not significantly alter the general behavior of the RF and RA models in $d=4+\epsilon$. As we shall see, it allows nonetheless to show that no Kosterlitz-Thouless-like transition occurs at the special point $(N_c, d=4)$ and that in the vicinity of this point, for $N<N_c$ and $d<4$, a once unstable fixed point appears, which describes the transition from the QLRO phase to the paramagnetic one. The picture is now fully compatible with that found in our NP-FRG approach and summarized in Fig. 1.

As for the one-loop level, it is worthwhile to start by considering the beta functions for the first two derivatives of the renormalized disorder correlator $R(z)=(\epsilon/C)\tilde{R}(z)$ evaluated in $z=1$, assuming that the second derivative is well-defined at that point. Writing the beta functions as $\beta=\beta_1+\beta_2$, we only give the expressions for the two-loop contributions β_2, the one-loop terms β_1 being given in Eqs. (33) and (34):

$$\epsilon^{-2} \beta_{\tilde{R}'(1),2} = (N-2) \tilde{R}'(1)^3, \tag{72}$$

$$\begin{aligned} \epsilon^{-2} \beta_{\tilde{R}''(1),2} = & \, 2(5N+17) \tilde{R}''(1)^3 + 6(N+7) \tilde{R}'(1) \tilde{R}''(1)^2 \\ & - 6(N-5) \tilde{R}'(1)^2 \tilde{R}''(1) - (N-4) \tilde{R}'(1)^3. \end{aligned} \tag{73}$$

One can immediately see that the fixed-point solution $\tilde{R}'_*(1) = \frac{1}{N-2}\left(1 - \frac{\epsilon}{N-2}\right)$ and its associated (positive) eigenvalue $\Lambda_1 = \epsilon\left(1 + \frac{\epsilon}{N-2}\right)$ lead to dimensional reduction, $\eta = \bar{\eta} = \eta_{DR}$

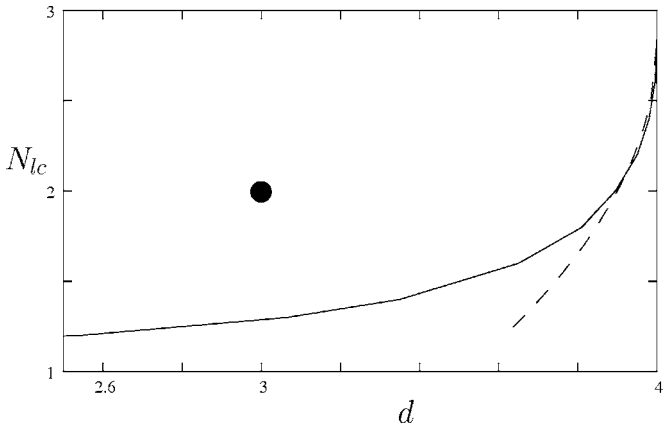

FIG. 12. Comparison between the results of the two-loop perturbative FRG (dashed line) and of the NP-FRG (continuous line) near $d=4$ for the QLRO lower critical dimension $N_{lc}(d)$ in the case of the RF$O(N)$M. The black circle denotes the physical case of the XY model in $d=3$, a case which is clearly below its lower critical dimension.

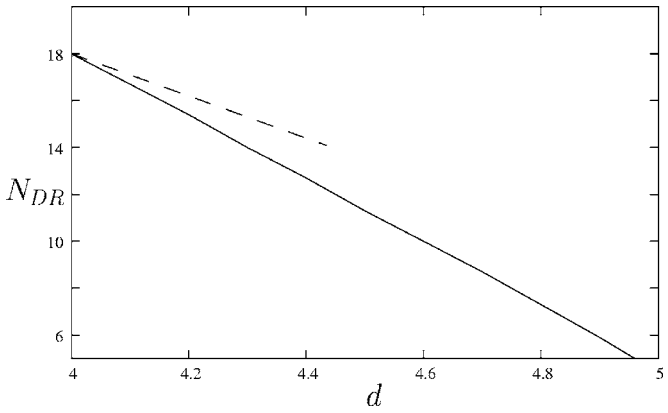

FIG. 13. Comparison between the results of the two-loop perturbative FRG (dashed line) and of the NP-FRG (continuous line) near $d=4$ for $N_{DR}(d)$ in the case of the RF$O(N)$M.

$=\frac{\epsilon}{(N-2)}\left(1+\frac{N-1}{N-2}\epsilon\right)$ [after using Eqs. (60) and (61)] and $\nu=\nu_{DR}=\frac{1}{\epsilon}-\frac{1}{N-2}$. When $\tilde{R}'(1)$ is chosen equal to its fixed-point value, the beta function for the second derivative becomes a cubic polynomial in $\tilde{R}''(1)$ which has zeros only if the associated discriminant is negative, i.e., if $N \geqslant 18-\frac{49}{5}\epsilon$.[27,30]

Following the same lines as for the one-loop order, one can check that the RF$O(N)$M at two loops has a critical fixed point with a "subcusp" when $N>N_{DR}=18-\frac{49}{5}\epsilon$, but that the critical fixed point of the RA$O(N)$M always has a cusp, implying $N_{DR}=\infty$ (see Appendix A).

We next concentrate on the region $N \leqslant N_c$ and $d \leqslant 4$. A first result is that the beta function for $R'(z)$ (unscaled by ϵ) in $d=4$ does not vanish for arbitrary values of the disorder strength $R'_*(1)$. When scaling out the disorder strength to define $r'(z)=R'(z)/R'_*(1)$, the beta function for $\epsilon=0$ can be expressed as $\beta_{r'}(z)=\beta_1[r',r']+R'_*(1)\beta_2[r',r',r']$. $\beta_{r'}(z)$ then vanishes independently of the value of $R'_*(1)$ if and only if $\beta_1[r',r']=0$ and $\beta_2[r',r',r']=0$ have the same solution $r'_*(z)$. It is straightforward to check that inserting the solution of the one-loop equation $\beta_1=0$ into the two-loop equation does not make the latter vanish identically. The consequence is that no Kosterlitz-Thouless transition can exist in $(N_c,d=4)$ since, even perturbatively, no line of fixed points can be found. Actually, the only fixed point at the two-loop level for $N=N_c$ and $d=4$ is the trivial one with $R'_*(1)=0$.

For $N \lesssim N_c$ and $d \lesssim 4$, consideration of the two-loop order brings in a new phenomenon. An additional, once unstable, fixed point appears, which describes the transition from the QLRO phase to the paramagnetic one. This new fixed point is found perturbatively in ϵ (which is now negative) and $N-N_c$. More precisely, as shown by Le Doussal and Wiese,[30] it can be obtained within a double expansion in $\sqrt{|\epsilon|}$ and $N-N_c$. For any given value of $N \lesssim N_c$, the critical fixed point and the QLRO fixed point get closer as $|\epsilon|$ increases and they merge for a value $\epsilon_{lc}(N)$. This latter corresponds to the lower critical dimension $d_{lc}=4+\epsilon_{lc}$ of QLRO. With the full two-loop results given above, Eqs. (56) and (69), one finds

$$d_{\mathrm{lc}}(\mathrm{RF}) = 4 - 0.14(N-N_c)^2 + \mathcal{O}[(N-N_c)^3], \qquad (74)$$

$$d_{\mathrm{lc}}(\mathrm{RA}) = 4 - 0.002(N-N_c)^2 + \mathcal{O}[(N-N_c)^3], \qquad (75)$$

where $N_c=2.8347\ldots$ for the RF model and $9.4412\ldots$ for the RA model. For what it is worth, directly plugging $N=2$ into the above expressions gives the following estimates for the lower critical dimension of the (QLRO) Bragg glass phase in the XY model: $d_{\mathrm{lc}}(\mathrm{RF}) \simeq 3.9, d_{\mathrm{lc}}(\mathrm{RA}) \simeq 3.9$. [Our NP-FRG theory predicts $d_{\mathrm{lc}}(\mathrm{RF}) \simeq 3.8$,[21] so that in all cases no Bragg glass is found for $N=2$ in $d=3$.]

Note that the fact that no Kosterlitz-Thouless transition takes place in $N=N_c$ and $d=4$ is connected to the absence of a linear term in $N-N_c$ in Eqs. (74) and (75). [In the pure $O(N)$ model on the contrary, $d_{lc}=2-b(2-N)+O[(N-2)^2]$, where $b=1/4$ is proportional to the temperature of the

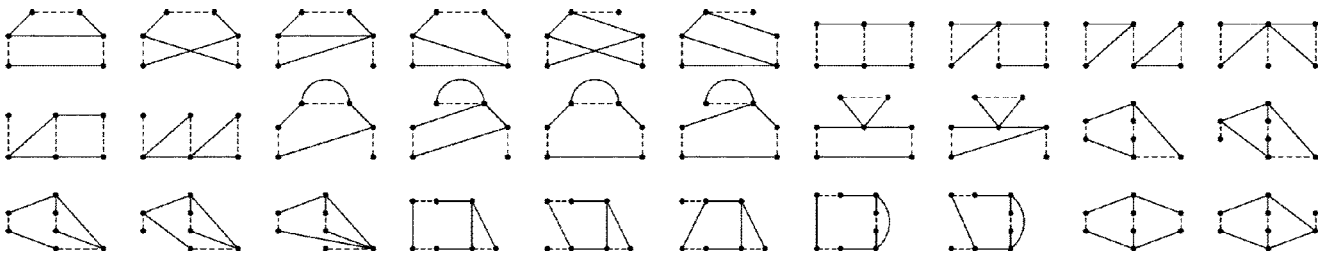

FIG. 14. Two-loop diagrams for the 2-replica effective action.

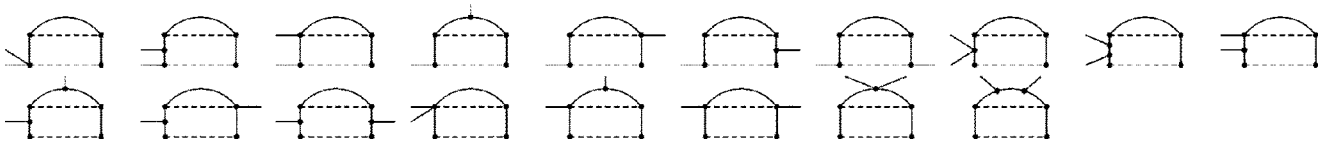

FIG. 15. Two-loop diagrams of type A for the 1-replica 2-point proper vertex.

Kosterlitz-Thouless transition.[31]] The slope of the curve $N_{lc}(d)$ giving the locus of the lower critical dimension for QLRO is infinite as $d \to 4^-$: see Fig. 12.

The two-loop predictions around $N=N_c$ and $N=N_{lc}(d)$ near $d=4$ are in agreement with those of our NP-FRG treatment. For a detailed comparison, we plot the two sets of results in Figs. 12 and 13. The nonperturbative, but approximate FRG computation does not exactly reproduce the two-loop calculation near $d=4$, but the differences are not very significant and do not alter the general picture.

To summarize: We have shown in this paper that the theory describing the long-distance physics of the RF and RA $O(N)$ models near $d=4$ is perturbatively renormalizable at two loops, thereby proving that the one-loop result is not fortuitous. The results we have obtained within the two-loop order fit into the general scenario predicted by our NP-FRG approach.[21,22] Considering the technical difficulties associated with the FRG loop expansion in $d=4+\epsilon$, it is highly unlikely that perturbative FRG will ever provide accurate extrapolations to the physical cases $d=2,3$ (and to $N=1$) for the RF and RA models. The NP-FRG on the other hand offers a direct way to study these situations.

APPENDIX A: FIXED POINTS AND THEIR STABILITY FOR THE RA$O(N)$M IN THE LARGE N LIMIT

We first rewrite the one-loop beta function for the derivative of $\tilde{T}(\phi)=(N-2)\tilde{R}(z)$, Eq. (40), by introducing the function $U(\phi)=-\tilde{T}'(\phi)/\sin\phi$,

$$\epsilon^{-1}\sin(\phi)\beta_U(\phi) = [U(0)-1]\sin(\phi)U(\phi) + [U(0)\cos(\phi)-U(\phi)]U'(\phi), \tag{A1}$$

and we look for fixed-point solutions. When $U_*(0)=1$, the only solutions are $U_*(\phi)=\cos\phi$ and $U_*(\phi)=1$. If $U_*(0)\neq 1$, the equation $\beta_U(\phi)=0$ can be solved by inverting the relation between U and ϕ and considering ϕ as a function of U. The fixed-point equation now reads

$$\partial_U[\cos\phi(U)] - \frac{U_0}{U_0-1}\frac{\cos[\phi(U)]}{U} = -\frac{1}{U_0-1}, \tag{A2}$$

where U_0 is such that $\phi(U_0)=0$. The solutions of Eq. (A2) are easily found as $\cos[\phi(U)]=KU^{U_0/(U_0-1)}+U$. K is a constant that is determined through the condition $\phi(U_0)=0$. The result can be reexpressed by stating that the fixed-point functions $U_*(\phi)$ are solutions of the following transcendental equation:

$$U_*(\phi) - [U_*(0)-1]\left(\frac{U_*(\phi)}{U_*(0)}\right)^{U_*(0)/(U_*(0)-1)} = \cos(\phi), \tag{A3}$$

where $U_*(0)$ is different from 1 but still unknown.

Note that the property $\tilde{T}(\pi-\phi)=\tilde{T}(\phi)$ imposes $U(\pi-\phi)=-U(\phi)$. Since we expect the functions to be analytic around $\frac{\pi}{2}$ (i.e., $z=0$), this property implies that $U(\frac{\pi}{2})$ and all even derivatives of U evaluated in $\frac{\pi}{2}$ are equal to zero. This requirement can only be fulfilled by the solutions of Eq. (A3) if $\frac{U_*(0)}{U_*(0)-1}$ is a nonzero integer. On the other hand, it cannot be satisfied by the solution $U_*(\phi)=1$, which should therefore be discarded.

To determine the acceptable values of $U_*(0)$, we have to turn to the stability analysis. Introducing a small deviation around the fixed point, $\delta(\phi)=U(\phi)-U_*(\phi)$, and linearizing the associated FRG equation leads to the following eigenvalue equation:

$$(\epsilon^{-1}\Lambda)\sin\phi\,\delta(\phi) = [\sin\phi U_*(\phi)+\cos\phi U_*'(\phi)]\delta(0) + \{[U_*(0)-1]\sin\phi - U_*'(\phi)\}\delta(\phi) + [U_*(0)\cos\phi - U_*(\phi)]\delta'(\phi). \tag{A4}$$

We first check that the solution $U_*(\phi)=\cos\phi$, corresponding to $U_*(0)=1$, is fully unstable with $\epsilon^{-1}\Lambda=1$, and we next consider the solutions given by Eq. (A3). As before we consider ϕ as a function of $U\equiv U_*(\phi)$, which gives after some manipulations,

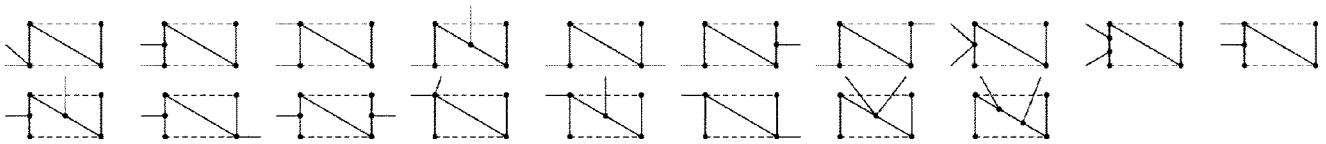

FIG. 16. Two-loop diagrams of type B for the 1-replica 2-point proper vertex.

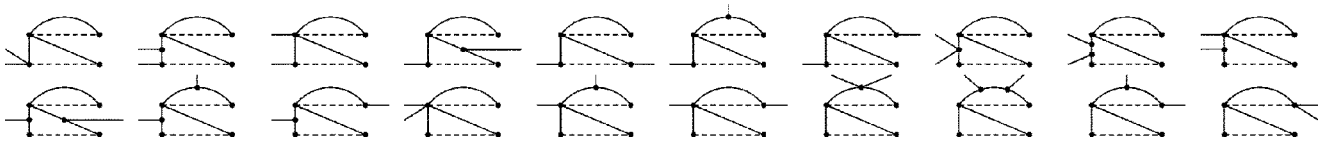

FIG. 17. Two-loop diagrams of type C for the 1-replica 2-point proper vertex.

$$\left(\frac{U}{U_0}\right)^{U_0/(U_0-1)}\delta(U_0) = -(U_0-1)\left[1-\left(\frac{U}{U_0}\right)^{1/(U_0-1)}\right]U\delta'(U) + \left\{1-(\epsilon^{-1}\Lambda-U_0+1)\times\left[1-\left(\frac{U}{U_0}\right)^{1/(U_0-1)}\right]\right\}\delta(U), \quad \text{(A5)}$$

where $U_0 \equiv U_*(\phi=0)$. The solution of the above equations is easily obtained as

$$\delta(U) = \frac{\delta(U_0)}{\epsilon^{-1}\Lambda}\left(\frac{U}{U_0}\right)^{(U_0-\epsilon^{-1}\Lambda)/(U_0-1)}\left[1-\left(\frac{U}{U_0}\right)^{\epsilon^{-1}\Lambda/(U_0-1)}\right]\times\left[1-\left(\frac{U}{U_0}\right)^{1/(U_0-1)}\right]^{-1}, \quad \text{(A6)}$$

where, we recall, $U_0/(U_0-1)$ is a nonzero integer. The condition that $\delta(U)$ be an odd fuction of U, analytic around $U=0$, imposes stringent constraints on $\epsilon^{-1}\Lambda$. One finds that the only singly unstable fixed point corresponds to $U_0/(U_0-1)=3$, i.e., $U_*(0)=3/2$. The associated eigenvalues are equal to $\epsilon^{-1}\Lambda=1,0,-1,-2,-3,\ldots$. For $U_*(0)=3/2$, Eq. (A3) can be explicitly solved, which leads to $U_*(\phi)=3\cos\left(\frac{\pi+\phi}{3}\right)$ and to Eq. (41).

To derive the fixed-point solution at the following orders in $1/N$, great simplification is obtained by first noticing that the above solution (in the limit $N\to\infty$) can be rewritten as

$$\tilde{T}'_*(\phi) = -\frac{3}{2}\sin\left(\frac{\pi-2\phi}{3}\right)\left[2\cos\left(\frac{\pi-2\phi}{3}\right)-1\right], \quad \text{(A7)}$$

which implies that $\tilde{T}_*(\phi)$ is a function of $\cos\left(\frac{\pi-2\phi}{3}\right)$. For finite N we now look for a fixed-point solution of the form $\tilde{T}'_*(\phi)=-\frac{3}{2}\sin\left(\frac{\pi-2\phi}{3}\right)(2X-1)G(X)$ with $X=\cos\left(\frac{\pi-2\phi}{3}\right)$. $G(X)$ can be expanded in powers of $1/N$ [or for convenience, $1/(N-2)$], its leading term being simply equal to 1 [see Eq. (A7)]. With this transformation the fixed-point equation can be solved in powers of $1/(N-2)$, each term being a polynomial in X. One obtains for the first terms

$$G(X) = 1+\frac{2}{9(N-2)}(95-44X-16X^2)+\mathcal{O}\left(\frac{1}{(N-2)^2}\right). \quad \text{(A8)}$$

From this expression, one derives $-T''_*(0)=\frac{3}{2}G\left(\frac{1}{2}\right)=\frac{3}{2}+\frac{23}{N}+O\left(\frac{1}{N^2}\right)$, which leads to the expressions given in Sec. III C.

Finally, the fixed point can also be found at the two-loop level in the large N limit by using the above variable X. One obtains, for instance, that the correlation length exponent is equal to

$$\nu = \frac{1}{\epsilon}-\frac{17}{3N}-\frac{29\,707}{81N^2}+\mathcal{O}\left(\frac{1}{N^3},\epsilon\right), \quad \text{(A9)}$$

so that it is now different from the dimensional-reduction value.

APPENDIX B: TWO-LOOP DIAGRAMS

Here we give all the two-loop diagrams built with the rules defined in Sec. IV A (see Figs. 14–20).

APPENDIX C: TWO-LOOP INTEGRALS IN DIMENSIONAL REGULARIZATION

In this section, we discuss the procedure used to evaluate the integrals appearing in the two-loop calculation in $d=4+\epsilon$.

1. Integrals for the 2-replica diagrams

We start with the integrals for the 2-replica effective action. The most general integral reads

$$J^{r,s,t}_{i,j,k,l,m,n}(a,b) = \int_{\mathbf{q}_1,\mathbf{q}_2,\mathbf{q}_3}\delta(\mathbf{q}_1+\mathbf{q}_2+\mathbf{q}_3)\times\frac{(\mathbf{q}_1\cdot\mathbf{q}_2)^r(\mathbf{q}_2\cdot\mathbf{q}_3)^s(\mathbf{q}_3\cdot\mathbf{q}_1)^t}{(q_1^2+a)^i(q_2^2+a)^j(q_3^2+a)^k(q_1^2+b)^l(q_2^2+b)^m(q_3^2+b)^n} \quad \text{(C1)}$$

with the parameters $\{i,j,k,l,m,n,r,s,t\}$ being nonnegative integers, $\{a,b\}$ being positive real numbers, and $r+s+t\leqslant 2$. The integrals have obvious symmetry properties since the

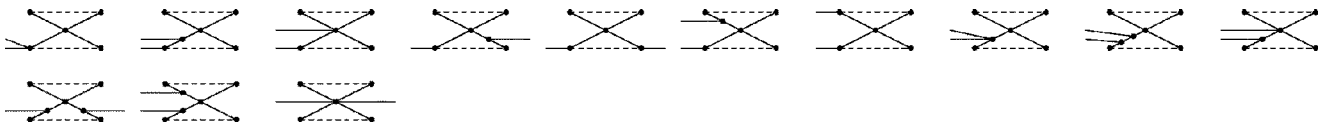

FIG. 18. Two-loop diagrams of type D for the 1-replica 2-point proper vertex.

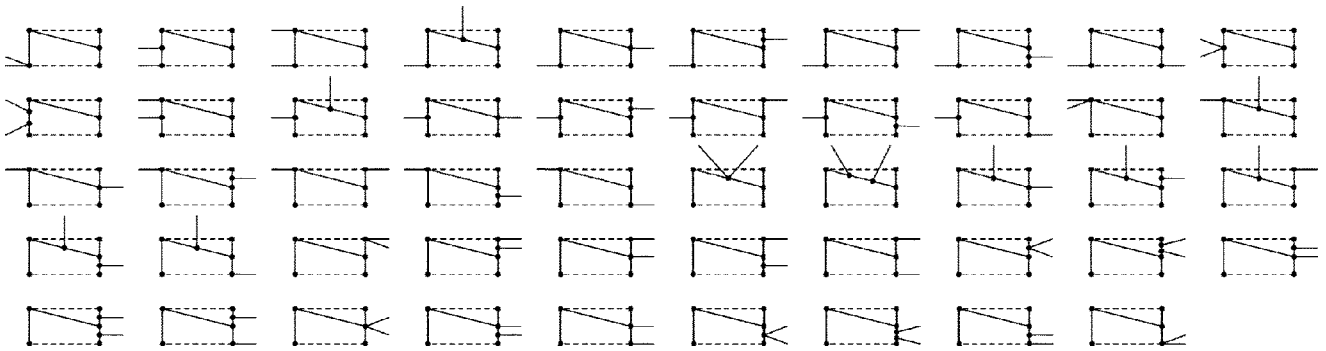

FIG. 19. Two-loop diagrams of type E for the 1-replica 2-point proper vertex.

integration variables can be exchanged. For instance, the integral is unchanged when $\{i,l,s\}$ and $\{j,m,t\}$ are exchanged, when $\{j,m,r\}$ and $\{k,n,t\}$ are exchanged, or when $\{i,j,k,a\}$ and $\{l,m,n,b\}$ are exchanged.

It is possible to reduce the range of values of $\{r,s,t\}$ that one must consider. This can be done by rewriting in the integrand $\mathbf{q}_1\cdot\mathbf{q}_2=(q_3^2-q_1^2-q_2^2)/2$; q_1^2 can then be replaced by $(q_1^2+a)-a$, which, if $i>0$, can be combined with $(q_1^2+a)^{-i}$ to give $(q_1^2+a)^{-i+1}-a(q_1^2+a)^{-i}$. Similar transformations can be done for q_2^2 and q_3^2. Then, under the assumption that i, j, and k are nonzero, one gets the identity

$$J^{rst}_{i,j,k,l,m,n}=\frac{1}{2}(J^{r-1,s,t}_{i,j,k-1,l,m,n}-J^{r-1,s,t}_{i,j-1,k,l,m,n}-J^{r-1,s,t}_{i-1,j,k,l,m,n}+aJ^{r-1,s,t}_{i,j,k,l,m,n}). \quad \text{(C2)}$$

Similar relations can be obtained under the (weaker) condition that $i+l$, $j+m$, and $k+n$ are nonzero.

There remains to treat the case where one of the three previous combinations (say, for instance, the last one) vanishes (which implies $k=n=0$). It is sufficient to treat the three cases where $\{r,s,t\}=\{1,0,0\}$ up to a permutation, because the other possibilities never appear in the calculation. Consider, for instance, $J^{100}_{i,j,0,l,m,0}$. Since q_3 appears in the integrand only through the δ function, one performs the integral on $\mathbf{q}_3$ trivially. The integrand can then be factorized in a piece $\mathbf{q}_1(q_1^2+a)^{-i}(q_1^2+b)^{-l}$ depending only on $\mathbf{q}_1$ and another (of a similar form) depending only on $\mathbf{q}_2$. Each piece is a vector so that the integral vanishes for symmetry reasons. Consider now the integral $J^{010}_{i,j,0,l,m,0}$. By integrating over $\mathbf{q}_3$, the numerator of the integrand becomes $-(q_2^2+\mathbf{q}_1\cdot\mathbf{q}_2)$. The last term gives zero after integration for symmetry reasons, just as before. The first term can be rewritten as $(q_2^2+a)-a$ so that, under the condition that $j>0$

$$J^{010}_{i,j,0,l,m,0}=aJ^{000}_{i,j,0,l,m,0}-J^{000}_{i,j-1,0,l,m,0}. \quad \text{(C3)}$$

Similar equations can be obtained if $j=0$ and $m>0$, or if $r=s=0$, $t=1$.

We can further simplify the integrals by using the relation

$$\frac{1}{(q^2+a)(q^2+b)}=\frac{1}{a-b}\left(\frac{1}{q^2+b}-\frac{1}{q^2+a}\right), \quad \text{(C4)}$$

which enables one to reduce the integrals to a form where, in the three couples $\{i,l\}$, $\{j,m\}$ $\{k,n\}$, at least one element is zero.

The previous procedure reduces the problem to the case $r=s=t=0$. In this case, the integral is finite (and therefore of no interest for us since we work in the minimal subtraction scheme) whenever the four conditions $i+j+k+l+m+n>4$, $i+j+l+m>2$, $j+k+m+n>2$, and $k+i+n+l>2$ are satisfied simultaneously. The divergent integrals can be of two types.

(1) If the smallest value between $i+l$, $j+m$, and $k+n$ is zero, then the integral factorizes and identifies to a product of one-loop integrals of the form

$$I_i(a)=\int_{\mathbf{q}}\frac{1}{(q^2+a)^i}=\frac{1}{(4\pi)^{d/2}}\frac{\Gamma(i-d/2)}{\Gamma(i)}a^{d/2-i}. \quad \text{(C5)}$$

(2) If the smallest value between $i+l$, $j+m$, and $k+n$ is 1, then the second smallest one must also be 1 for the integral to be divergent, and the last one is free. All these integrals can be calculated by using derivatives of the relation

$$\int_{\mathbf{q}_1\mathbf{q}_2\mathbf{q}_3}\frac{\delta(\mathbf{q}_1+\mathbf{q}_2+\mathbf{q}_3)}{(q_1^2+a)(q_2^2+b)(q_3^2+c)}=-C\frac{a^{d-3}+b^{d-3}+c^{d-3}}{d-3}\left(\frac{1}{2\epsilon^2}-\frac{1}{4\epsilon}\right)+\mathcal{O}(\epsilon^0) \quad \text{(C6)}$$

with $C^{-1}=8\pi^2$.

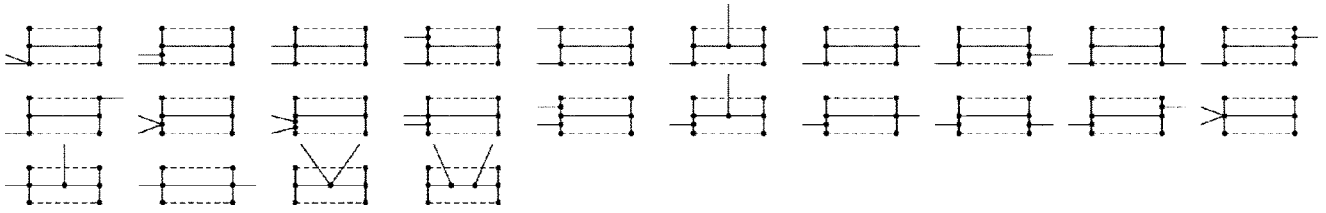

FIG. 20. Two-loop diagrams of type F for the 1-replica 2-point proper vertex.

2. Integrals for the 1-replica diagrams

The situation for the 1-replica diagrams is in a sense simpler because only one mass can appear. However, the vertices and propagators can now come with the external momentum $\mathbf{p}$. The first step in the evaluation of the integrals consists in expanding the integrand in powers of $\mathbf{p}$, keeping only the constant, linear, and quadratic terms which are of interest in the renormalization procedure. The linear part of the integral vanishes for symmetry reasons. The constant part can be evaluated by using the procedure described in the previous section.

The quadratic part can come in the two following forms: p^2 or $(\mathbf{q}_i\cdot\mathbf{p})(\mathbf{q}_j\cdot\mathbf{p})$. The first case is simple and can be evaluated by using the procedure described above. For the second form, we used the relation

$$\int_{\mathbf{q}_1\mathbf{q}_2\mathbf{q}_3} \delta(\mathbf{q}_1+\mathbf{q}_2+\mathbf{q}_3)(\mathbf{q}_i\cdot\mathbf{p})(\mathbf{q}_j\cdot\mathbf{p})f = \frac{p^2}{d}\int_{\mathbf{q}_1\mathbf{q}_2\mathbf{q}_3} \delta(\mathbf{q}_1+\mathbf{q}_2+\mathbf{q}_3)(\mathbf{q}_i\cdot\mathbf{q}_j)f, \tag{C7}$$

where f is a function of $\mathbf{q}_1$, $\mathbf{q}_2$, and $\mathbf{q}_3$ and i,j are equal to 1, 2, or 3. The case $i\neq j$ can then be treated as in the previous section. In the case $i=j$, the integrand always comes with $(q_i^2+c)^\alpha$ in the denominator, so one can use again the relation

$$\frac{q_i^2}{(q_i^2+c)^\alpha} = \frac{1}{(q_i^2+c)^{\alpha-1}} - \frac{c}{(q_i^2+c)^\alpha} \tag{C8}$$

and compute the remaining part by using the procedure described previously.

*Electronic address: tissier@lptl.jussieu.fr
†Electronic address: tarjus@lptl.jussieu.fr

[1] D. P. Belanger, *Spin Glasses and Random Fields* (World Scientific, Singapore, 1998), p. 258.
[2] F. Brochard and P. G. de Gennes, J. Phys. (France) Lett. **44**, L785 (1983).
[3] P. G. de Gennes, J. Phys. Chem. **88**, 6469 (1984).
[4] E. Pitard, M. L. Rosinberg, G. Stell, and G. Tarjus, Phys. Rev. Lett. **74**, 4361 (1995).
[5] T. Giamarchi and P. Le Doussal, *Spin Glasses and Random Fields* (World Scientific, Singapore, 1998), p. 277.
[6] G. Blatter, M. V. Feigel'man, V. B. Geshkenbern, A. I. Larkin, and V. M. Vinokur, Rev. Mod. Phys. **66**, 1125 (1994).
[7] T. Nattermann and S. Scheidl, Adv. Phys. **49**, 607 (2000).
[8] T. Giamarchi and P. Le Doussal, Phys. Rev. Lett. **72**, 1530 (1994).
[9] T. Giamarchi and P. Le Doussal, Phys. Rev. B **52**, 1242 (1995).
[10] R. Harris, M. Plischke, and M. J. Zuckermann, Phys. Rev. Lett. **31**, 160 (1973).
[11] M. Dudka, R. Folk, and Y. Holovatch, J. Magn. Magn. Mater. **294**, 305 (2005).
[12] D. E. Feldman, Int. J. Mod. Phys. B **15**, 2945 (2001).
[13] Y. Imry and S. K. Ma, Phys. Rev. Lett. **35**, 1399 (1975).
[14] J. Bricmont and A. Kupiainen, Phys. Rev. Lett. **59**, 1829 (1987).
[15] A. I. Larkin, Sov. Phys. JETP **31**, 784 (1970).
[16] M. Aizenman and J. Wehr, Phys. Rev. Lett. **62**, 2503 (1989).
[17] J. Z. Imbrie, Phys. Rev. Lett. **53**, 1747 (1984).
[18] T. Nattermann, *Spin Glasses and Random Fields* (World Scientific, Singapore, 1998), p. 277.
[19] D. S. Fisher, Phys. Rev. B **31**, 7233 (1985).
[20] D. E. Feldman, Phys. Rev. B **61**, 382 (2000).
[21] M. Tissier and G. Tarjus, Phys. Rev. Lett. **96**, 087202 (2006).
[22] G. Tarjus and M. Tissier, Phys. Rev. Lett. **93**, 267008 (2004).
[23] D. S. Fisher, Phys. Rev. Lett. **56**, 1964 (1986).
[24] P. Le Doussal and K. J. Wiese, Phys. Rev. Lett. **89**, 125702 (2002).
[25] P. Le Doussal, K. J. Wiese, and P. Chauve, Phys. Rev. E **69**, 026112 (2004).
[26] D. E. Feldman, Phys. Rev. Lett. **88**, 177202 (2002).
[27] Y. Sakamoto, H. Mukaida, and C. Itoi, Phys. Rev. B **74**, 064402 (2006).
[28] E. Brézin and J. Zinn-Justin, Phys. Rev. B **14**, 3110 (1976).
[29] M. Schwartz and A. Soffer, Phys. Rev. Lett. **55**, 2499 (1985).
[30] P. Le Doussal and K. J. Wiese, Phys. Rev. Lett. **96**, 197202 (2006).
[31] J. L. Cardy and H. W. Hamber, Phys. Rev. Lett. **45**, 499 (1980).
[32] For some values of N, $\alpha(N)$ may accidentally be an integer, but logarithmic corrections should be present in this case.
[33] Note that, in the two-loop calculation, one must keep the one-loop contributions that are finite [of order $O(\epsilon^0)$] because these terms, when the replacements defined in Eqs. (12) are made, are multiplied by the one-loop counterterms in $1/\epsilon$ and therefore contribute to the singular part.
[34] This value corresponds to the lower bound given in Refs. 27 and 28 of Ref. 30.